



**CALIFORNIA  
ENERGY COMMISSION**



**CALIFORNIA  
natural  
resources  
AGENCY**

Energy Research and Development Division

## **FINAL PROJECT REPORT**

# **Characterization of Snowpack and Snowmelt Runoff in High-Elevation Remote Basins**

**Improving the Characterization of California's  
Snowpack for Water and Energy Resource  
Management**

**March 2023 | CEC-500-2023-027**

**PREPARED BY:**

**Primary Author:**

Steven A. Margulis

University of California, Los Angeles  
5732D Boelter Hall  
Los Angeles, CA 90095  
310-267-5490  
www.ucla.edu

**Contract Number:** 300-15-006-04

**PREPARED FOR:**

California Energy Commission

Brad Williams

**Project Manager**

Virginia Lew

**Office Manager**

**ENERGY EFFICIENCY RESEARCH OFFICE**

Jonah Steinbuck, Ph.D.

**Deputy Director**

**ENERGY RESEARCH AND DEVELOPMENT DIVISION**

Drew Bohan

**Executive Director**

**DISCLAIMER**

This report was prepared as the result of work sponsored by the California Energy Commission. It does not necessarily represent the views of the Energy Commission, its employees or the State of California. The Energy Commission, the State of California, its employees, contractors and subcontractors make no warranty, express or implied, and assume no legal liability for the information in this report; nor does any party represent that the uses of this information will not infringe upon privately owned rights. This report has not been approved or disapproved by the California Energy Commission nor has the California Energy Commission passed upon the accuracy or adequacy of the information in this report.

## PREFACE

The California Energy Commission's (CEC) Energy Research and Development Division supports energy research and development programs to spur innovation in energy efficiency, renewable energy and advanced clean generation, energy-related environmental protection, energy transmission and distribution and transportation.

In 2012, the Electric Program Investment Charge (EPIC) was established by the California Public Utilities Commission to fund public investments in research to create and advance new energy solutions, foster regional innovation and bring ideas from the lab to the marketplace. The CEC and the state's three largest investor-owned utilities—Pacific Gas and Electric Company, San Diego Gas & Electric Company and Southern California Edison Company—were selected to administer the EPIC funds and advance novel technologies, tools, and strategies that provide benefits to their electric ratepayers.

The CEC is committed to ensuring public participation in its research and development programs that promote greater reliability, lower costs, and increase safety for the California electric ratepayer and include:

- Providing societal benefits.
- Reducing greenhouse gas emission in the electricity sector at the lowest possible cost.
- Supporting California's loading order to meet energy needs first with energy efficiency and demand response, next with renewable energy (distributed generation and utility scale), and finally with clean, conventional electricity supply.
- Supporting low-emission vehicles and transportation.
- Providing economic development.
- Using ratepayer funds efficiently.

*Characterization of Snowpack and Snowmelt Runoff in High-Elevation Remote Basins* is the final report for the Characterization of Snowpack and Snowmelt Runoff in High-Elevation Remote Basins project (Contract Number 300-15-006) conducted by the University of California, Los Angeles. The information from this project contributes to the Energy Research and Development Division's EPIC Program.

For more information about the Energy Research and Development Division, please visit the [CEC's research website](http://www.energy.ca.gov/research/) (www.energy.ca.gov/research/) or contact the CEC at ERDD@energy.ca.gov.

# ABSTRACT

The Sierra Nevada in California provides not only most of the state's water supply but also a significant portion of its energy supply via hydroelectric power. Existing hydropower systems are optimized for historical runoff patterns that are changing under long-term climate warming. Snow-dominated basins are particularly susceptible to changes in runoff regime (more rainfall versus less snowfall and earlier snowmelt). These effects have the potential to drastically change the hydrograph characteristics in river basins that supply hydropower. This project focused on developing an improved characterization of snow-dominated basins that contribute to water and hydropower supply. The primary objective was to understand the accumulation and melt of snow in these watersheds and how they contribute to runoff by developing a historical retrospective database (that is, snow reanalysis) over the Landsat remote sensing record (1985 – present). A "snow reanalysis" framework was used to characterize the climatology and variability of snow water resources over the study domain and the remote sensing record. The new database was then used as a mechanism to test new frameworks for predicting streamflow from these watersheds, assess climate models that are used for forecasting snowpack water resources, assess how runoff from these watersheds may evolve under climate change, and develop and test a new real-time algorithm for estimating snow accumulation and melt in these remote basins from newly available remote sensing products. The project results provide a new database for public use and indicate the potential for new tools to improve snow-derived streamflow forecasting from Sierra Nevada watersheds at a variety of lead times. Implementing such frameworks will have direct economic benefits by allowing for improvements in streamflow predictions and hydroelectric power forecasts and management.

**Keywords:** snow, remote sensing, runoff, streamflow, hydroelectric power, rain-on-snow, climate change

Please use the following citation for this report:

Margulis, Steven. 2023. *Characterization of Snowpack and Snowmelt Runoff in High-Elevation Remote Basins*. California Energy Commission. Publication Number: CEC-500-2023-027.

# TABLE OF CONTENTS

Page

PREFACE .....	i
ABSTRACT .....	ii
TABLE OF CONTENTS .....	iii
LIST OF FIGURES .....	iv
EXECUTIVE SUMMARY .....	1
Introduction.....	1
Project Purpose.....	1
Project Approach.....	1
Project Results .....	2
Technology/Knowledge Transfer/Market Adoption (Advancing the Research to Market).....	2
Benefits to California .....	3
CHAPTER 1: Introduction .....	4
CHAPTER 2: Project Approach .....	6
2.1 Development of Sierra Nevada Snow Reanalysis Dataset .....	6
2.1.1 Application Domain: Sierra Nevada Watersheds .....	6
2.1.2 Snow Estimation (Reanalysis) Method .....	7
2.1.2 Data Needed for Snow Reanalysis and Verification .....	8
2.2 Testing the Effect of Improved Snow Estimates on Runoff Forecasts .....	9
2.2.1 Hydrologic Modeling Framework .....	9
2.2.2 Snow-Water Equivalent Initialization and Forecast Experimental Method .....	<b>Error!</b>
<b>Bookmark not defined.</b>	
2.3 Evaluation of Climate Models in Representing Sierra Nevada and Western United States Snowpack Estimates.....	11
2.3.1 Variable-Resolution Community Earth System Model .....	11
2.3.2 Geophysical Fluid Dynamics Laboratory Atmosphere-Ocean General Circulation Modeling Framework .....	12
2.4 Role of Rain-on-Snow on Snowmelt-Driven Runoff in Current and Future Climates .....	13
2.5 Examination of Real-Time Snow Estimation Method .....	14
CHAPTER 3: Project Results.....	16
3.1 Sierra Nevada Snow Reanalysis .....	16
3.2 Testing the Effect of Improved Snow Estimates on Runoff Forecasts .....	20

3.3 Evaluation of Climate Models in Representing Sierra Nevada and Western United States Snowpack Estimates .....	23
3.3.1 Variable-Resolution Community Earth System Model .....	23
3.3.2 Geophysical Fluid Dynamics Laboratory Atmosphere-Ocean General Circulation Modeling Framework .....	25
3.4 Role of Rain-on-Snow on Snowmelt-Driven Runoff in Current and Future Climates .....	27
3.5 Examination of Real-Time Snow Estimation Method .....	31
CHAPTER 4: Technology/Knowledge/Market Transfer Activities.....	36
CHAPTER 5: Conclusions and Recommendations.....	37
CHAPTER 6: Benefits to Ratepayers .....	39
REFERENCES .....	40

## **LIST OF FIGURES**

	Page
Figure 1: California’s Precipitation and Hydropower Distribution .....	4
Figure 2: Sierra Nevada Domain and Its Characteristics.....	7
Figure 3: Snow Reanalysis Framework .....	8
Figure 4: California Watershed Forecast Points .....	10
Figure 5: Variable Resolution Climate Model application over California .....	12
Figure 6: Climate Model Snow-Water Equivalent Over Western United States .....	13
Figure 7: United States Domain Used in Rain-on-Snow Experiments.....	14
Figure 8: Tuolumne River Watershed Data .....	15
Figure 9: Verification of Snow Reanalysis Against In-Situ Data.....	17
Figure 10: Illustrative Maps of Snow Reanalysis Snow-Water Equivalent.....	18
Figure 11: Seasonal and Interannual Variability in Rangewide Snow-Water Equivalent .....	19
Figure 12: Streamflow Forecast Comparison for Merced River.....	20
Figure 13: Streamflow Forecast Evaluation for All Basin-Years .....	21
Figure 14: Streamflow Forecast Comparison for All Basin-Years Compared to Operational Forecasts.....	22
Figure 15: Forecast Improvement Relative to Operational Forecasts.....	22
Figure 16: Forecast Improvement Relative to Operational Forecasts in Dry Years.....	23
Figure 17: Climate Model Snow-Water Equivalent Difference Maps.....	24

Figure 18: Climate Model Seasonal Snow-Water Equivalent Differences.....	25
Figure 19: Climate Model Snow-Water Equivalent Over Western United States (2012-2015) ..	26
Figure 20: Statistical Performance of Climate Model Prediction Skill .....	27
Figure 21: Verification of Snow-Water Equivalent in Rain-on-Snow Simulations.....	29
Figure 22: Historical Rain-on-Snow Event Characterization .....	30
Figure 23: Future Changes in Rain-on-Snow Events .....	31
Figure 24: Illustration of Prior, Measurement, and Posterior Snow Depth.....	32
Figure 25: Estimation Errors in Snow Depth for All Measurement Times .....	33
Figure 26: Peak Snow-Water Equivalent and Snowmelt Time Series .....	35

# EXECUTIVE SUMMARY

## Introduction

California's climate is dominated by a strong seasonal cycle in precipitation, in which most of the precipitation falls in the winter with strong spatial variations between northern and southern portions of the state and between coastal and mountain regions. Much of the precipitation that falls in winter is in the form of snow, and a large portion of California's population relies on snowmelt for a majority of its water supply and a significant amount (around 19 percent) of energy from hydroelectric power. These snowpack-derived water/energy resources are located in remote mountain terrain that, despite having arguably the densest monitoring network in the United States, has a relatively sparse in-situ sampling. Models based on this in-situ data often rely on underlying assumptions of statistical stationarity that are being eroded by climate change. Hence, characterizing these water and hydropower energy resources, and how they are changing, requires a paradigm shift away from relying solely on scarce in-situ data and moving toward novel remote sensing observations and modeling tools.

## Project Purpose

This project focused on developing an improved characterization of snow-dominated basins that contribute to water and hydropower supply. The primary objective was to understand the accumulation and melt of snow in these watersheds and how they contribute to runoff by developing a historical retrospective database over the Landsat satellite remote sensing record (1985 – present). The snow reanalysis was used to characterize the climatology and variability of snow-water resources over the study domain and the remote sensing record. Other key objectives of the project involved using the new database as a mechanism to test new frameworks for predicting streamflow from these watersheds, assess climate models that are used for predicting and/or forecasting snowpack water resources, assess how runoff from these watersheds may change under climate change, and develop and test a new real-time algorithm for estimating snow accumulation and melt in these remote basins from newly available remote sensing products. Based on this work, stakeholders that manage hydroelectric power infrastructure, could improve their forecasts to better manage energy generation.

## Project Approach

The project researchers used remote sensing data and numerical snow, hydrology, and climate models to analyze Sierra Nevada snow resources and how those resources are evolving and expected to vary in the future. The specific approach involved the following key elements: 1) developing a novel Sierra Nevada snow reanalysis dataset; 2) testing the effect of improved snow estimates from the dataset on runoff forecasts; 3) evaluating climate models' effectiveness in representing Sierra Nevada snowpack estimates and predicting seasonal lead times; 4) evaluating the role of rain-on-snow events on snowmelt-driven runoff in the current and future climate; and 5) developing and analyzing a new real-time snow estimation method based on newly available remotely sensed snow depth. This set of studies provided a comprehensive analysis of snow-derived runoff from the Sierra Nevada and how its prediction

can be improved. The methods involve computational techniques that will be more robust to accommodate for the lack of in-situ data and climate change predictions.

## **Project Results**

Project results tied to the key elements described above include:

1. Development of the new state-of-the-art Sierra Nevada snow reanalysis dataset, which is based on the use of retrospective Landsat data and compares favorably to in-situ data. The dataset is currently available for public use by any interested stakeholders and provides a unique capability for investigating snow processes at a space-time resolution, temporal extent, and accuracy not available from other existing datasets.
2. Demonstration of how streamflow forecast models could benefit significantly from realistic snow fields like those in the dataset. Winter-time initialization of such models with realistic snow estimates increased the accuracy of operational statistical forecasts by 13 percent across all years and by 23 percent in dry years with earlier initialization. Such improvements would pay significant dividends on streamflow and, therefore, hydropower forecasts.
3. Evaluation of snow estimation and prediction by two different climate modeling frameworks, which found that: a) higher resolution models additionally require improved precipitation models to best predict snow distribution in space and time and b) the Sierra Nevada is a particularly difficult domain for making long lead-time (that is, eight month) predictions due to the narrowness of the mountain range compared to some coarse scale climate models.
4. Evaluation of the current effect of rain-on-snow in generating runoff and streamflow that showed the significant impact of such events in the Sierra Nevada, including extreme runoff events in spring. Evaluation of rain-on-snow events in a future warmer climate highlighted the amplified role of rain-on-snow in local streamflow extremes in high-elevation mountains like the Sierra Nevada.
5. Development of a new framework for real-time snow-water equivalent and snowmelt-driven runoff from remotely sensed snow depth measurements. In particular, the research team found that even a single measurement of snow depth around April 1 can provide useful estimates of snow-water equivalent and snowmelt during the rest of the melt season, suggesting the cost of such new measurement systems could accrue significant benefits.

## **Technology/Knowledge Transfer/Market Adoption (Advancing the Research to Market)**

In this project, the research team developed a new snow dataset to analyze snow-derived water resources in California's Sierra Nevada. The researchers used the new dataset in conjunction with modeling studies to characterize how snow-water equivalent, and therefore snow-derived runoff, can be improved. The dataset and model results are available and were provided to stakeholders to provide a better understanding of the historical and future availability of these resources. This project was part of a larger United States Department of Energy Clean Energy Research Center for Water-Energy Technologies project (<https://cerc-wet.berkeley.edu/>). As part of that larger effort, the research team participated in regular

industry and stakeholder outreach (see <https://cerc-wet.berkeley.edu/events>) that presented results to a wide audience including relevant stakeholders. The analysis provides valuable information for policy makers and stakeholders in preparing future climate adaptation plans about how changes in snow-derived runoff may affect changes in hydropower production and optimal management. The researchers will continue to work with the California Energy Commission and other hydroelectric power stakeholders to provide information based on the analysis in this report.

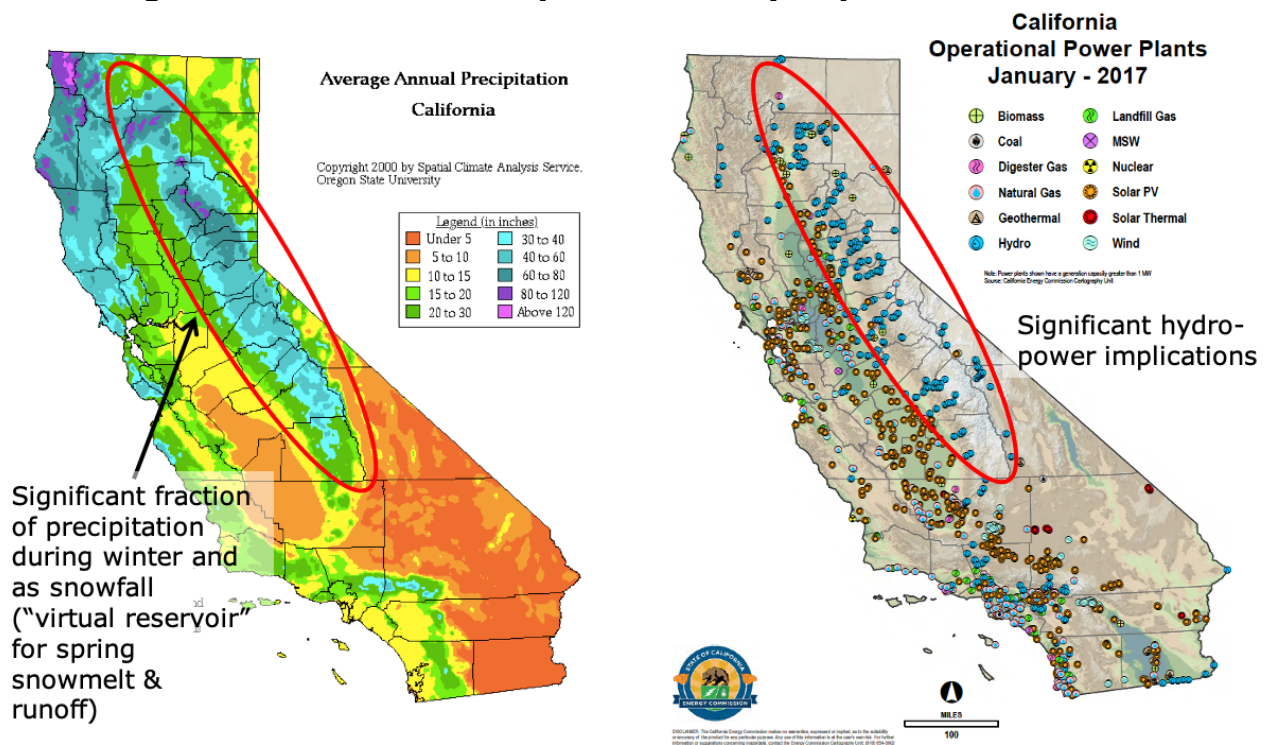
## **Benefits to California**

This project has benefitted ratepayers by developing new datasets, analyses, and tools needed to better characterize Sierra Nevada snowpack and thereby improve streamflow forecasts for hydropower at various lead times, and how those forecasts are likely to change under long-term climate warming. Using the conclusions and recommendations in this project, California can be better equipped to optimally manage snow-derived water and energy resources in the future. Developing and implementing such frameworks will have direct economic benefits by allowing for improvements in streamflow predictions and hydroelectric power forecasts and management.

# CHAPTER 1: Introduction

California’s climate is dominated by a strong seasonal cycle in precipitation, in which most of the precipitation falls in the winter with strong spatial variations between northern and southern portions of the state and between coastal and mountain regions (Figure 1). Much of the precipitation that falls in winter does so in the form of snow, and a large portion of California’s population relies on snowmelt for a majority of its water supply and a significant amount (about 19 percent) of energy from hydroelectric power (Figure 1). These snowpack-derived water/energy resources are located in remote mountain terrain that, despite having the densest monitoring network in the United States, has a relatively sparse in-situ sampling. For example, the Sierra Nevada has a snow pillow network that samples less than 1 percent of the snow-dominated area (Guan et al., 2013), much of which is concentrated at middle elevations, leaving most high-elevation regions completely unsampled. Moreover, models based on this in-situ data often rely on underlying assumptions of statistical stationarity that are being eroded by climate change (Milly et al., 2008). Characterizing these water and hydropower energy resources, and how they are changing, requires a paradigm shift away from relying solely on scarce in-situ data.

**Figure 1: California’s Precipitation and Hydropower Distribution**



**Distribution of precipitation in California (left), showing significant portion as snowfall over the Sierra Nevada along with the large number of hydropower plants (right) that use streamflow from these headwater basins.**

Source: PRISM (Oregon State University) and California Energy Commission

While the effect of climate change on precipitation is complex and poorly understood, models are in agreement that temperature will continue increasing in the future with a multitude of effects on California and its resources (Bedsworth et al., 2018). This temperature signal makes snow-dominated basins particularly susceptible to changes in runoff regime: Some fraction of precipitation that traditionally fell as snow will instead fall as rain. Warmer temperatures will also drive earlier snowmelt. These two effects have the potential to drastically change the hydrograph characteristics in high-elevation river basins that provide water and hydropower supply. Existing hydropower systems are optimized for historical runoff patterns. Consequently, changes in runoff volumes and/or timing has the potential to affect hydropower in unknown ways.

This project focused on developing an improved characterization of snow-dominated basins that contribute to water and hydropower supply. Application areas focus primarily on the Sierra Nevada of California and the broader Western United States where snow plays an outsized role. The primary objective is to understand the accumulation and melt of snow in these watersheds and how they contribute to runoff by developing a historical retrospective database (that is, "snow reanalysis") over the Landsat remote sensing record (1985 – present). The snow reanalysis is used to characterize the climatology and variability of snow-water resources over the study domain and the remote sensing record of approximately the last 30 years. The new database is then used as a mechanism to test new frameworks for predicting streamflow from these watersheds, assessing climate models that are used for predicting and/or forecasting snowpack water resources, assessing how runoff from these watersheds may change under climate change, and developing and testing a new real-time algorithm for estimating snow accumulation and melt in these remote basins from newly available remote sensing products. These individual studies are organized as follows:

1. Development of the Sierra Nevada Snow Reanalysis (SNSR) dataset.
2. Testing the effect of improved snow estimates on runoff forecasts.
3. Evaluation of climate models in representing Sierra Nevada and Western United States snowpack estimates and their prediction.
4. The role of rain-on-snow on snowmelt-driven runoff in the current and future climate.
5. Examination of a real-time snow estimation method.

The results of this work are described in the subsequent sections of this report and in more detail in Margulis et al. (2016a, b; 2019), Kapnick et al. (2018), Rhoades et al. (2018), and Li et al. (2019a, b). These studies lay the groundwork for future work to adopt the use of the datasets and methods for improving California water and power supply forecasting at sub-seasonal to seasonal lead times.

# CHAPTER 2:

## Project Approach

---

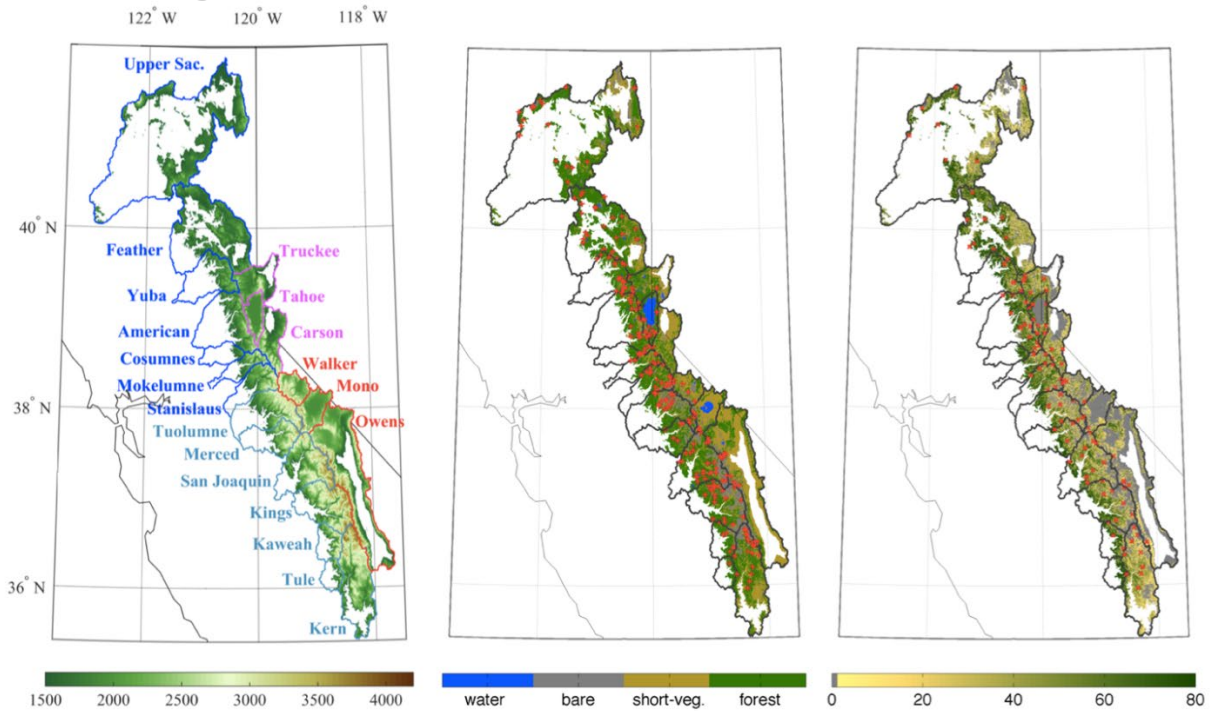
### **2.1 Development of Sierra Nevada Snow Reanalysis Dataset**

The first study in this project was the development of a new snow dataset that forms the basis for much of the work that follows. The domain and methodology are described below.

#### **2.1.1 Application Domain: Sierra Nevada Watersheds**

As a first step, the Sierra Nevada Snow Reanalysis (SNSR) dataset was developed over the key snow-dominated watersheds in the Sierra Nevada spanning California and Nevada in the Western United States (Figure 2). Specifically, the domain of interest included watersheds on the western slope (that is, from Upper Sacramento in the north to Kern in the south) along with Owens and Mono basins on the eastern slope that supply water to California. The remaining watersheds on the eastern slope (that is, from Truckee in the north to Walker in the south) generally drain to lakes including Lake Tahoe and others in the Great Basin. The watersheds in the Sierra Nevada span elevations from a few hundred meters above mean sea-level to 4,421 meters (Mount Whitney in the Kern River watershed). The reanalysis dataset was developed for these 20 watersheds and is applied to elevations above 1,500 meters (m), which represent the nominal snow line, and covers 49,409 kilometers (km).<sup>2</sup> The range-wide and basin-wise distribution of elevation, landcover, and fractional forest cover are illustrated in Figure 2.

**Figure 2: Sierra Nevada Domain and Its Characteristics**



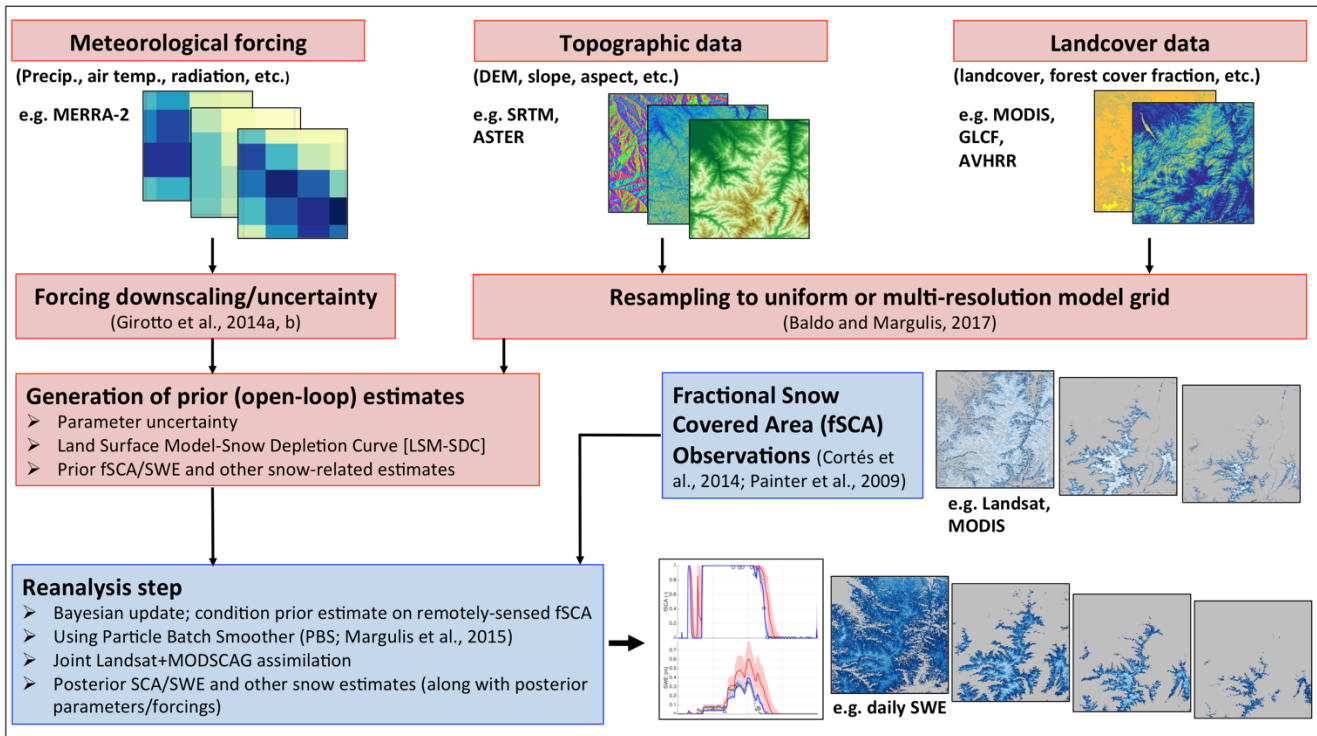
Maps of (left) elevation (in meters) over the domain (including watershed outlines/names), (middle) landcover type, and (right) forest cover fraction (percent). Location of snow courses and snow pillows are shown respectively with red symbols in (middle) and (right).

Source: University of California, Los Angeles

### 2.1.2 Snow Estimation (Reanalysis) Method

The estimation (reanalysis) method applied herein (Figure 3) consists of a Bayesian approach called the particle batch smoother, which was developed and validated in Margulis et al. (2015). The method can be summarized as follows: 1) A model is used to first generate an initial guess (that is, the prior estimate), which is then 2) updated by remotely sensed fractional snow-covered area (fSCA) observations to generate a final (posterior) estimate. The prior estimate leverages readily available high-resolution elevation and landcover data as static inputs, and downscaled meteorological forcing (Giroto et al., 2014a; Margulis et al., 2015) as the time-varying inputs, to generate high-resolution snow-water equivalent (SWE) estimates over the full water year (WY), October 1 – September 30. The method accounts for uncertainty in key model inputs, including the downscaled meteorological variables (Giroto et al., 2014a, b; Margulis et al., 2015). The approach is a fully probabilistic Bayesian method that provides daily SWE estimates at 90 m resolution. A more detailed description of the method is provided in Margulis et al. (2015; 2019a).

**Figure 3: Snow Reanalysis Framework**



Schematic representation of the Bayesian snow reanalysis framework that consists of an ensemble-based prior modeling system (red boxes) and a posterior update component for assimilating remotely sensed fractional snow-covered area.

Source: University of California, Los Angeles

### 2.1.2 Data Needed for Snow Reanalysis and Verification

Static model inputs for the prior modeling system (Xue et al., 2003; Liston, 2004) consisted of 30 m resolution elevation and landcover information from the ASTER (<http://asterweb.jpl.nasa.gov/>) and NLCD (Homer et al., 2007) databases. These inputs were aggregated to 90 m resolution for use in the reanalysis. The hourly meteorological inputs used were taken from the 1/8° resolution NLDAS-2 dataset (Xia et al., 2012) and were downscaled probabilistically to 90 m based on topographic corrections and uncertainty models (Giroto et al., 2014a, b; Margulis et al., 2015).

The retrieved fSCA estimates used in this study were derived from Landsat 5 Thematic Mapper, Landsat 7 Enhanced Thematic Mapper, and Landsat 8 Operational Land Imager reflectance data (Painter et al., 2003; Cortés et al., 2014). Based on data availability, only Landsat 5 was used from WY 1985–1998, Landsat 5 and 7 were used from WY 1999–2011, Landsat 7 was used solely in WY 2012, and Landsat 7 and 8 were used in WY 2013–2015.

The data used for verification in this study is in-situ SWE data taken from 108 snow pillow and 202 snow course sites scattered across the Sierra Nevada. The quality-controlled data is available from the Department of Water Resources California Data Exchange Center (<http://cdec.water.ca.gov/>). Snow pillows provide daily measurements, while snow courses provide monthly measurements near the first of each month from January through May. Many of the snow courses are co-located with snow pillows. The spatial distribution and basin-

specific number of verification sites in the Sierra Nevada are shown in Figure 2. Validation of the SNSR dataset and representative results are shown in Section 3.1.

## **2.2 Testing the Effect of Improved Snow Estimates on Runoff Forecasts**

The second study in this project was aimed at understanding how a high-resolution and accurate SWE product would affect seasonal streamflow forecast skill. The SNSR was used as a representative example of such a dataset. The method used is described below.

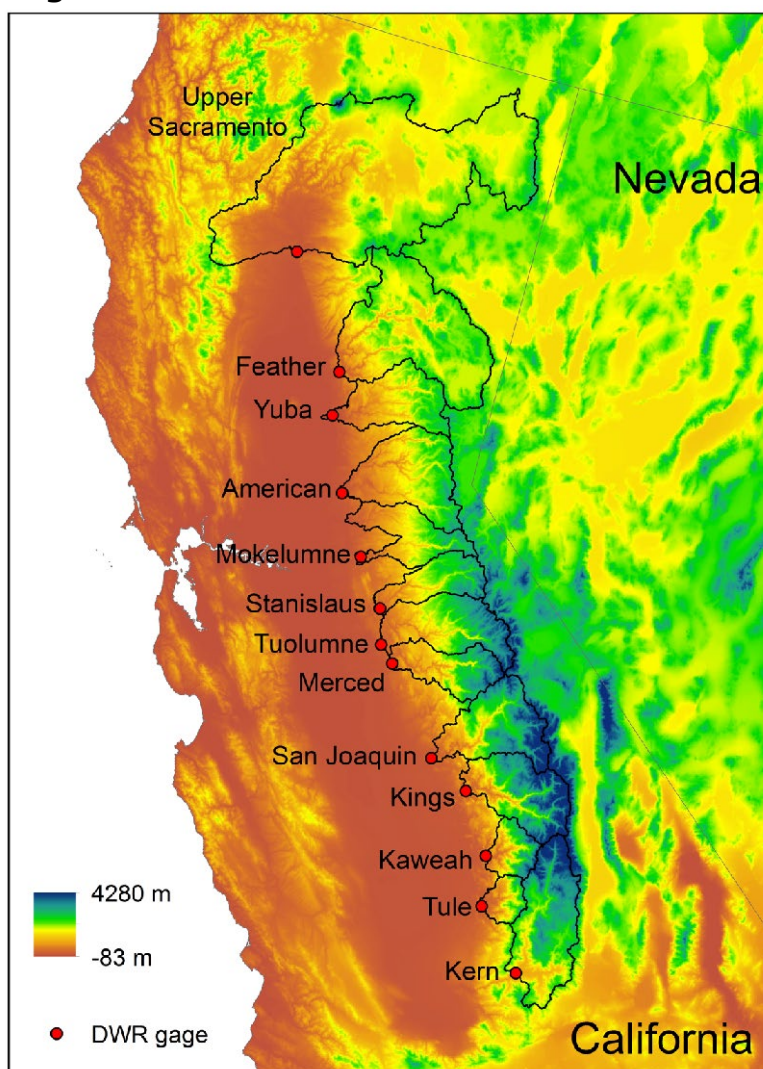
### **2.2.1 Hydrologic Modeling Framework**

The validated SNSR provides a realistic spatially distributed snow dataset that can be used to assess whether having such information would provide skill improvement in streamflow forecasts. To test the effect of improved snow characterization on runoff, the Variable Infiltration Capacity (VIC) hydrology model (Liang et al., 1994) was used. The model was setup to forecast at the outlets of the 13 river basins draining the western slopes of the Sierra Nevada (Figure 4). The model was applied at its commonly applied spatial resolution of 1/16 degree latitude/longitude (about 6 km) with an hourly temporal resolution for the 31-year period from 1985 to 2015. The VIC model has been well-calibrated for the California basins where the modeled streamflow has a high degree of agreement with observations (Maurer et al., 2002; Livneh et al., 2013). No additional model calibration was performed for this study. The modeling framework was used for both baseline and test simulations, where the former was meant to represent the potential effect of forecasts under a normal scenario and the latter, a scenario with improved snow representation. In the context of this study, the method was applied as a series of annual hindcasts where baseline and validation data are available.

### **2.2.2 Snow-Water Equivalent Initialization and Forecast Experimental Method**

To assess the effect of improved snow representation, the SNSR data on the day of peak SWE (typically around April 1) was used to re-initialize the basin snow conditions in the baseline simulation on that day. The only difference between the baseline forecast and test forecast was the difference in SWE initial conditions. Going forward in time from the re-initialization, the streamflow from the forecasting framework therefore reflects the effect of the inserted (SNSR) SWE initial condition. It was hypothesized that the new initial SWE condition would immediately reduce the error of the modeled SWE, allowing for the exploration of the extent to which the improved SWE affects the accuracy of the seasonal streamflow forecasts.

**Figure 4: California Watershed Forecast Points**



**Map showing the 13 headwater river basins with forecast points (gages) shown as red dots at which the California Department of Water Resources produces seasonal streamflow forecasts. The VIC model is applied upstream of each forecast point.**

Source: University of California, Los Angeles

Two streamflow forecast experiments—a perfect forecast and a standard ensemble streamflow prediction (ESP)—were applied. In the perfect forecast, the VIC model was forced with the observed historical gridded meteorological data for that year. Thus, the perfect forecast is an ideal scenario that allows for the assessment of the best possible forecast the system could produce, given the actual realization of the forcing during the forecasting period (Wood et al., 2016). In comparison, ESP reproduces a more realistic forecasting scenario in which the meteorological conditions during the forecast period are unknown, and a forcing ensemble is used to characterize the meteorological dynamics and uncertainty during the forecast period.

The perfect forecasting and the ESP used identical forcing data (the same as used in the SNSR); each has an insertion (SWE reinitialization) forecast and a baseline forecast. The analysis included two streamflow comparisons: 1) baseline versus re-initialized SWE forecasts and 2) re-initialized SWE versus operational California Department of Water Resources (DWR) streamflow forecasts compared to observed streamflow. The former comparison is analogous

to previous work (Kumar et al., 2013; Liu et al., 2015) and was done primarily to identify whether the re-initialization of SWE is a dominant factor in streamflow and can thereby improve streamflow forecasts. The latter comparison was done to assess the overall accuracy of the re-initialization of SWE compared to an operational framework. Representative results from these forecasts tests are provided in Section 3.2. More details on the experimental and modeling setup are provided in Li et al. (2019a).

## **2.3 Evaluation of Climate Models in Representing Sierra Nevada and Western United States Snowpack Estimates**

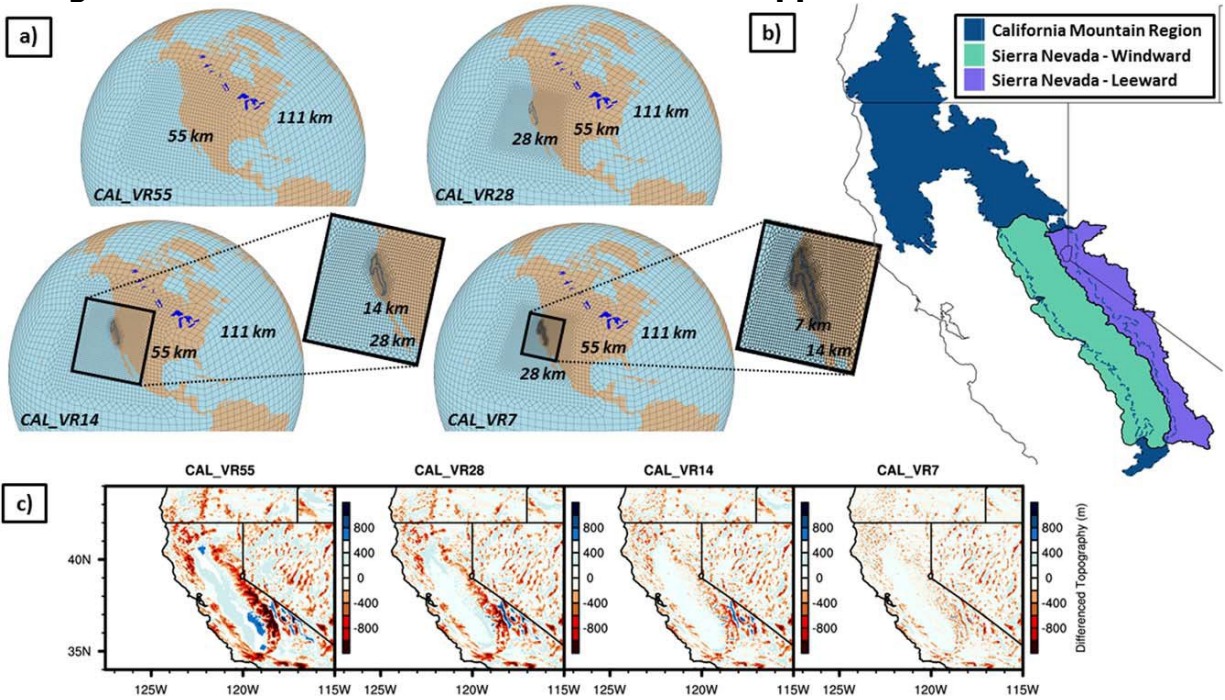
Climate models will increasingly be the tools used to diagnose, forecast, and project snow-derived water and energy resources in areas like California and the Western United States. However, until recently, verification and evaluation of such tools has been difficult due to lack of compatible and accurate snow datasets. The SNSR developed as part of this project was used in comparisons with two different climate models as described below to assess the potential of such models in predicting and forecasting Sierra Nevada SWE.

### **2.3.1 Variable-Resolution Community Earth System Model**

The Variable-Resolution Community Earth System Model (VR-CESM) is comprised of stand-alone atmospheric, land-surface, oceanic, sea-ice, and land-ice components. A detailed description of the benefits of VR-CESM are given in Zarzycki et al. (2015) and Rhoades et al. (2016, 2017). However, one key aspect of VR-CESM relevant to this study is that the variable-resolution allows a global model to “zoom in” to mountainous areas at higher resolutions (Figure 5).

The two key aspects of climate models with respect to simulations in mountain regions are resolution and the so-called microphysics parameterization of clouds and precipitation. Together these two factors are key to resolving the orographic-driven precipitation and snowfall that are characteristic of mountain regions. To examine the joint effect of these two factors, eight VR-CESM simulations were conducted for this study (over the period 1999 – 2015): 1) at refined horizontal resolutions over California of 55 km, 28 km, 14 km, and 7 km and 2) using two different microphysics parameterizations (Morrison and Gettelman, 2008 [MG1] and Gettelman and Morrison, 2015 [MG2]). These topography-microphysics combinations are expected to yield differences in snowfall and snowmelt (among many other factors). Representative results from these simulation cases and how they compare to SNSR are provided in Section 3.3.1. More details on the experimental and modeling setup are described in Rhoades et al. (2018).

**Figure 5: Variable Resolution Climate Model Application Over California**



VR-CESM grid used for this study showing: a) uniform global grid with grid refinement in California at resolutions of 55 km, 28 km, 14 km, and 7 km; b) regions of analysis in California; and c) topographic differences at varying resolutions.

Source: University of California, Los Angeles

### 2.3.2 Geophysical Fluid Dynamics Laboratory Atmosphere-Ocean General Circulation Modeling Framework

To study another aspect of snow simulation and predictability, the Geophysical Fluid Dynamics Laboratory (GFDL) atmosphere-ocean general circulation model, or AOGCM, (Delworth et al., 2006) was used to test the lead-time predictability of Western United States snowpack. Three versions of the AOGCM were applied that differ in their horizontal atmospheric/land resolutions (that is, 200 km, 50 km, and 25 km; Figure 6). Seasonal eight-month lead-time predictions that were initialized on July 1 for the subsequent March Western United States snowpack were derived from three AOGCM multimember ensemble hindcasts (Kapnick et al., 2018). Starting from these July 1 initial conditions, the dynamical model then predicted the evolution of the climate system over the following year, allowing for the assessment of predicted snowpack values for the following March (1981–2016). Model results used ensemble mean predictions. Simpler statistical models were also tested by using observed climate indices available on July 1 to contrast with the dynamical AOGCM predictions. The dynamical physical models and statistical models were verified against snow-water equivalent (SWE) observations and reanalysis including the SNSR over the Sierra Nevada. Representative results from these simulation cases are provided in Section 3.3.2. More details on the experimental and modeling setup are described in Kapnick et al. (2018).

**Figure 6: Climate Model Snow-Water Equivalent Over Western United States**

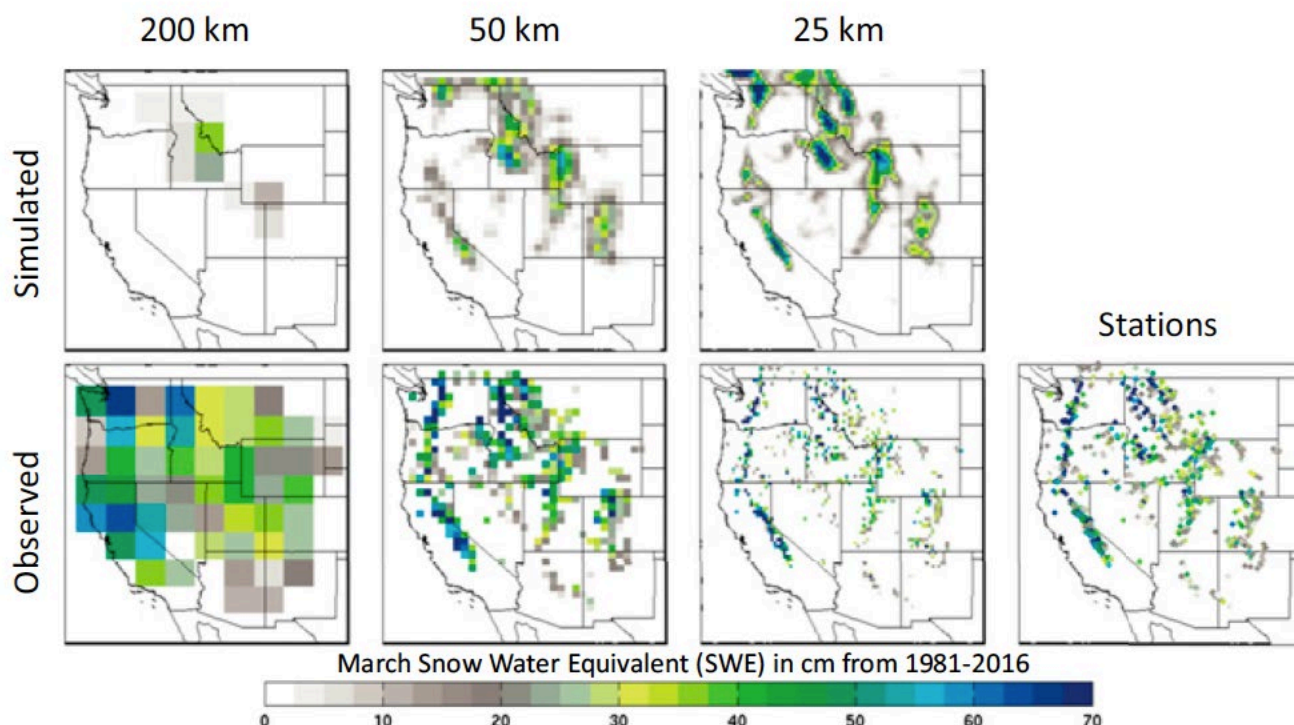


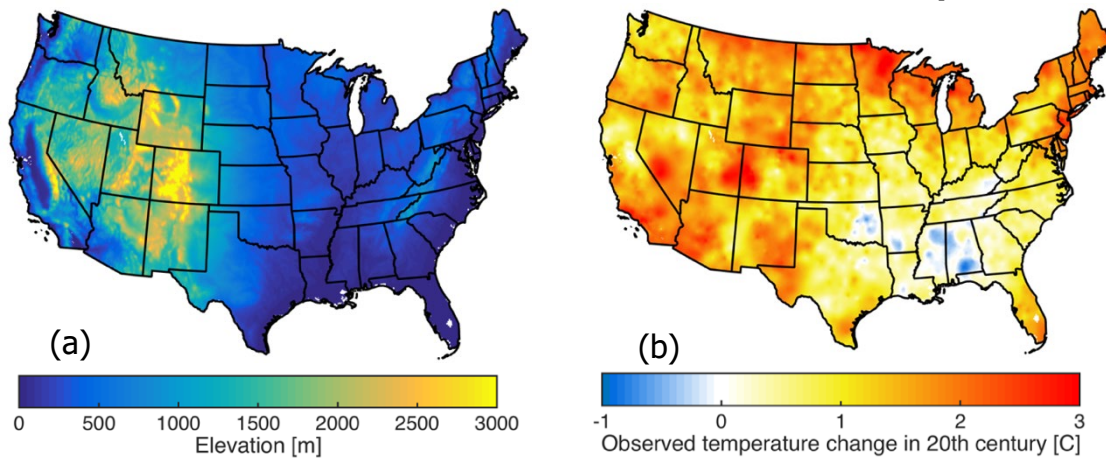
Illustration of the GFDL AOGCM model at different resolutions (200 km, 50 km, and 25 km) in terms of simulated climatological SWE (top row) versus observed SWE (bottom row). The Western United States observations shown here are based on in-situ station data (bottom right) that are regridded.

Source: University of California, Los Angeles

## 2.4 Role of Rain-on-Snow on Snowmelt-Driven Runoff in Current and Future Climates

Rain-on-snow is a potentially important component of current and future runoff. In this study, the same VIC model setup described in Section 2.2.1 was used to characterize flood risk associated with rain-on-snow (ROS) events both in the current climate and in how they are likely to change under climate warming. In this study, the domain of application was the broader conterminous United States (CONUS), as shown in Figure 7, over the 64-year period covering 1950–2013. Flood risk was based on VIC-simulated runoff using the Generalized Extreme Value, or GEV, (Cheng et al., 2014) distribution. To define ROS days, the criteria in Freudiger et al. (2014) was used. This method defines an ROS day as one having at least 3 millimeters (mm) of rain falling on a snowpack with at least 10 mm SWE, and for which snowmelt makes up at least 20 percent of the sum of the rainfall and snowmelt for the day. In this study the criteria were used to identify every ROS day over the 64-year study period at each grid cell. After identifying the ROS days for all grid cells, the ROS frequency in days per year was calculated along with the centroid of timing of the ROS days based on the rainfall intensity-weighted average of the ROS timing in days of the water year (WY; that is, days from 1 October). This method was applied to the historical period and then applied to the case with the warming scenario. Representative results from this analysis are provided in Section 3.4. More details on the experimental and modeling setup are described in Li et al. (2019b).

**Figure 7: United States Domain Used in Rain-on-Snow Experiments**



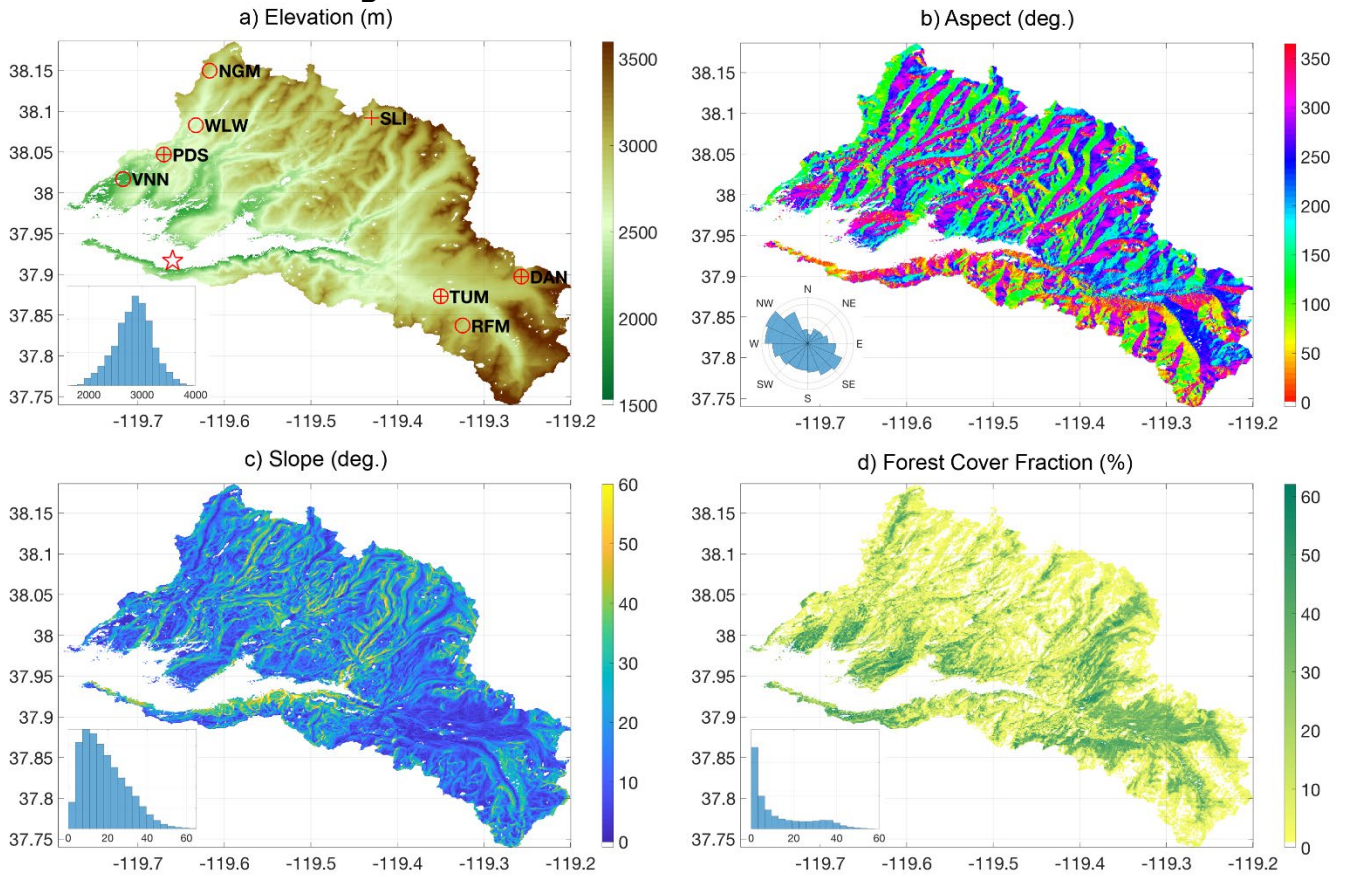
**(a) Elevation of the CONUS study domain. (b) Observed temperature change in the 20<sup>th</sup> century (1991 – 2012 average compared to the 1901–1960 average). The mean temperature increased by about 34.1°F (1.2°C) on average over the domain (data source: Third National Climate Assessment, Melillo et al., 2014).**

Source: University of California, Los Angeles

## 2.5 Examination of Real-Time Snow Estimation Method

Finally, to examine how real-time SWE estimates could be made, the same data assimilation framework used in the development of the SNSR was used with newly available LIDAR-based Airborne Snow Observatory, or ASO, (Painter et al., 2016) snow depth (SD) dataset. The SNSR dataset is only available retrospectively (that is, for historical purposes after all snow disappears) because fSCA data does not provide instantaneous information about SWE. However, SD is closely related to SWE and therefore opens up the possibility of real-time SWE estimation. The research team focused on the Tuolumne River basin in the Sierra Nevada of California (Figure 8) where ASO data is available. The ASO snow depth dataset provides multitemporal lidar-derived SD images per year over this watershed, compared to most lidar datasets that only provide one SD estimate per year. The researchers used the ASO dataset as a testbed to assess how well a single SD image per year would perform in generating spatially and temporally continuous SWE estimates. Data was used from three water years (WYs): 2015 (historically dry), 2016 (near average), and 2017 (historically wet). The baseline case assimilated a single SD image from ASO that was taken on the Day of Water Year (DOWY) closest to April 1 in each WY (DOWYs 185 in 2015, 184 in 2016, and 183 in 2017). A sensitivity test was also performed to assess how results change with respect to the number of assimilated measurements. Representative results from these tests are provided in Section 3.5. More details on the experimental and modeling setup are described in Margulis et al. (2019b).

**Figure 8: Tuolumne River Watershed Data**



Maps showing the spatial distribution of key physiographic characteristics across the Tuolumne basin: a) elevation, b) aspect, c) slope, and d) forest cover. Insets in each subpanel show the binned frequency distribution of each variable within the basin. Sites with in-situ snow data are shown in panel a) as either snow course sites ('o') or snow pillow sites ('+'). The location of the United States Geological Survey stream gage is identified with a red star.

Source: University of California, Los Angeles

# CHAPTER 3:

## Project Results

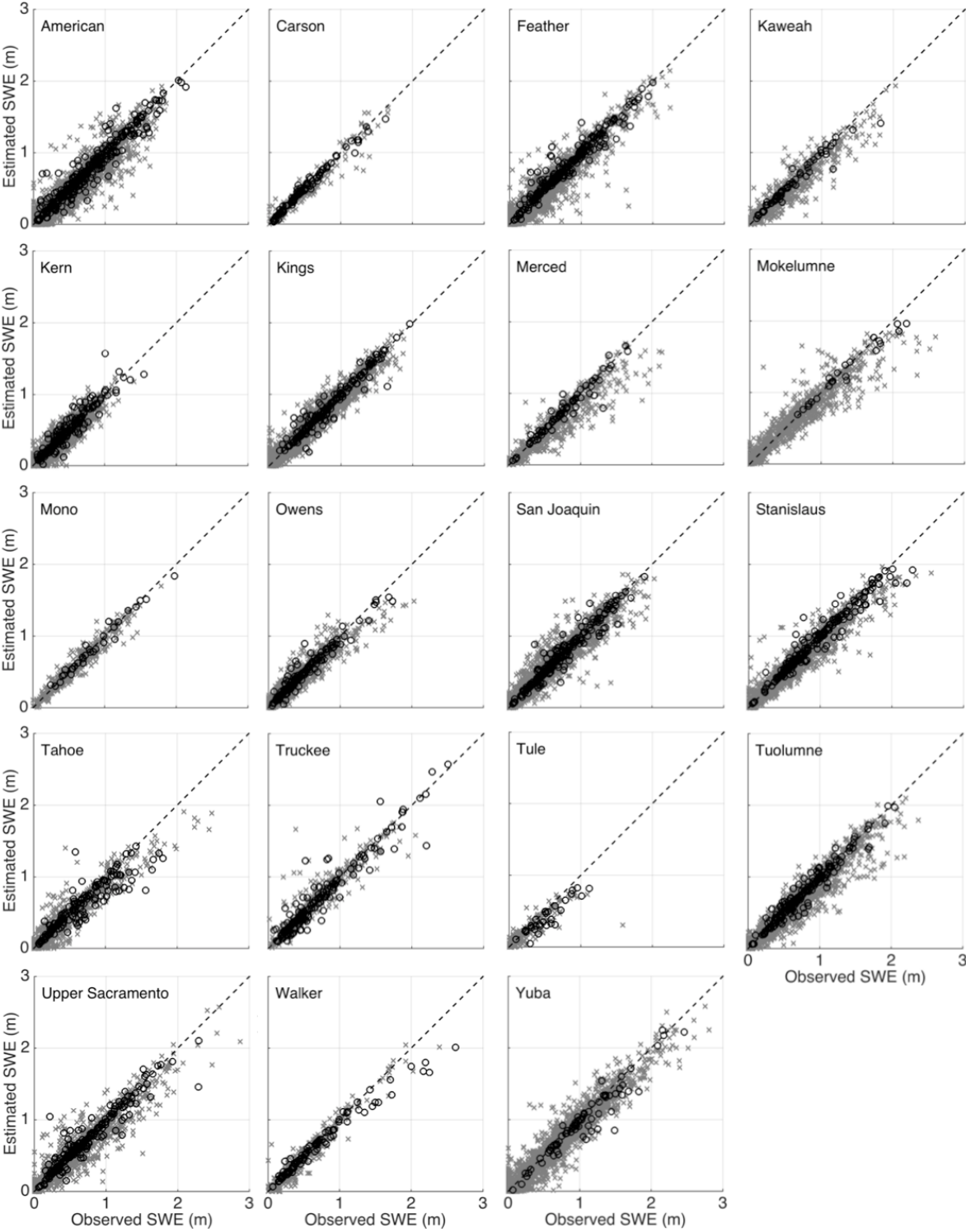
---

### 3.1 Sierra Nevada Snow Reanalysis

The SNSR estimates were compared to all snow pillow and snow course sites across California as a means of verification. Scatter plots showing the comparison of posterior estimates to observations are shown in Figure 9 and visually confirm the general agreement between the estimates and observations. For snow pillow data, the verification was performed on the peak SWE values. For the snow course data, the verification was performed for all data (typically at the beginning of the month between January and May). The comparison performed includes more than 9,000 station-years of data. The posterior SWE estimates are generally significantly improved over the prior estimates in terms of mean error, root-mean-squared error (RMSE), and correlation coefficient when compared to the in-situ data. The posterior mean error values for snow pillows range from -12 – 1 centimeter (-1 centimeter [cm] across all sites). The posterior RMSE values for snow pillows values range from 5 – 18 cm (11 cm across all sites). The posterior correlation coefficient values for snow pillows range from 0.91 – 0.99 (0.97 across all sites). The results are qualitatively similar for snow courses, with uniform and significant improvement in all metrics across all basins (with posterior mean error, RMSE, and correlation coefficient across all sites of -3 cm, 13 cm, and 0.95 respectively). These estimation errors compare favorably to other methods (Margulis et al., 2016).

To highlight the SNSR SWE estimates that were derived as part of this study, Figure 10 (left panel) illustrates the climatological average (31-year average over 1985 – 2015 water years) reanalysis map of peak range-wide SWE over the domain. The patterns of spatial variability show the clear signature of larger SWE values at higher elevations and on the windward (western) slopes of the range. The average climatological SWE over the domain is 0.38 m. For context, the 2015 drought year SWE map is shown in Figure 10 (right panel) and illustrates how much less SWE occurred; the average SWE over the domain is 0.06 m (about 16 percent of the climatological average). In addition to the significantly lower SWE depth in 2015, many more pixels showed zero SWE values at the time of range-wide peak. Specifically, while the climatology map has SWE values of zero in 2 percent of the non-water covered portion of the domain, 47 percent of the domain had zero SWE values in 2015.

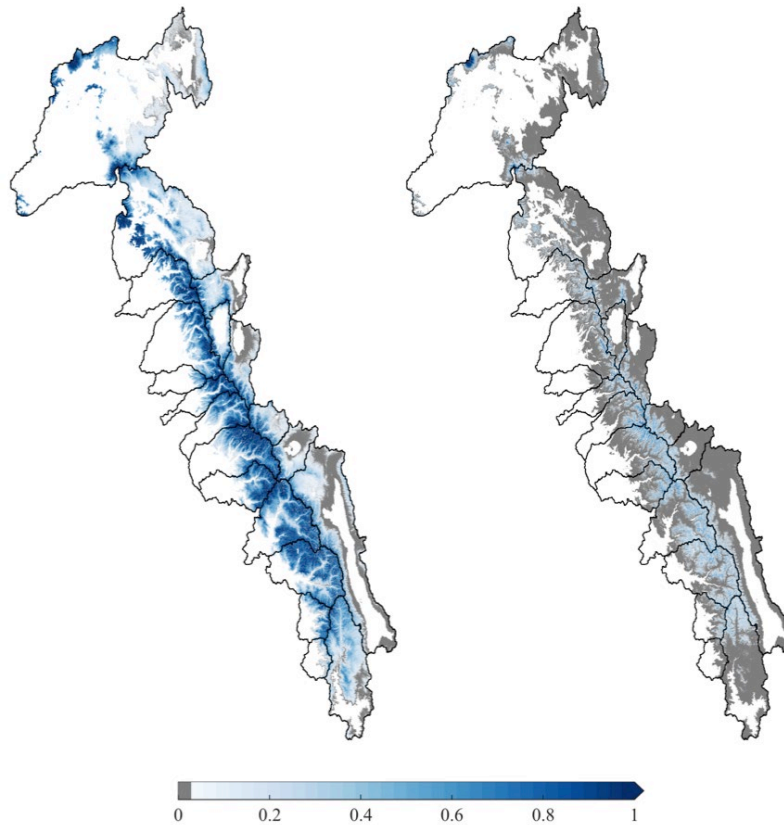
**Figure 9: Verification of Snow Reanalysis Against In-Situ Data**



**Comparison of observed SWE to posterior SWE reanalysis estimates at snow pillow (black 'o' symbols) and snow course (grey 'X' symbols) locations.**

Source: University of California, Los Angeles

**Figure 10: Illustrative Maps of Snow Reanalysis Snow-Water Equivalent**



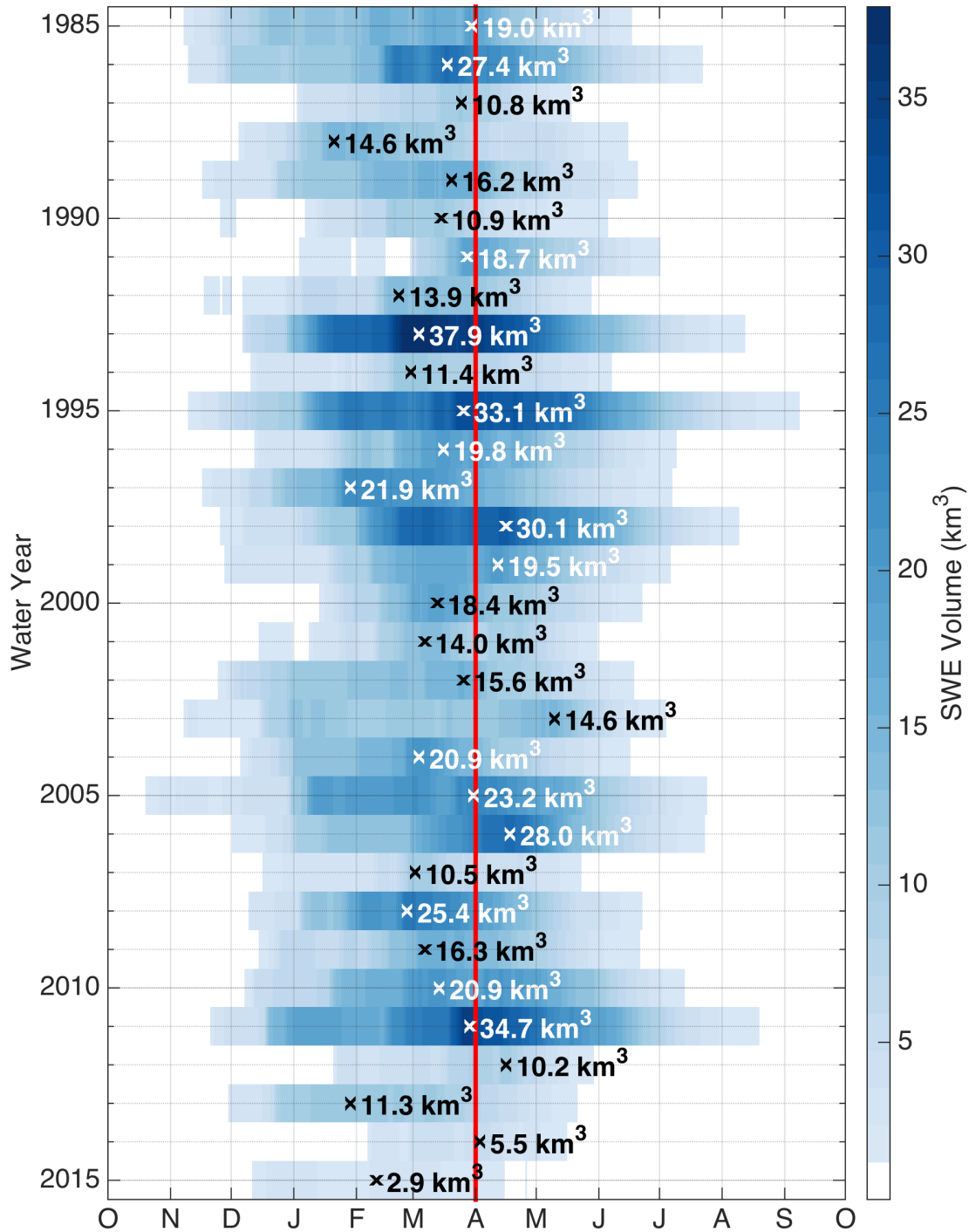
**Maps of snow-water equivalent (in meters) on day of range-wide peak snow-water equivalent volume corresponding to: (left panel) 31-year climatology and (right panel) water year 2015. White areas in the maps indicate those regions outside of the reanalysis domain (water bodies and areas below 1,500 m).**

Source: University of California, Los Angeles

As a final example of the insight that can be gained from the reanalysis, Figure 11 provides a comprehensive illustration of the range-wide SWE dataset as a function of both WY and day of WY. The strong seasonal cycle and inter-annual variability is evident in the dataset, which shows a range in the peak SWE from 2.9 – 37.9 km<sup>3</sup> with an average of 18.6 km<sup>3</sup>. It is also clear from Figure 11 that the timing of peak SWE varies significantly. While the average day of range-wide peak SWE is March 15, the inter-annual day-of-peak ranges from January 20 – May 9. Considering the actual date of peak is important as evidenced by 2015, where the peak is quite early (February 10) and much of the snow is melted by April 1. Hence using April 1 to quantify variations in peak SWE has the potential to introduce significant errors and in the case of 2015 makes what is already an extreme year seem even more so.

More details on the SNSR can be found in Margulis et al. (2016a, b) and the data can be found at <https://margulis-group.github.io/data/>. Based on the development of the dataset and its positive performance, it was used in the subsequent studies related to snow-derived runoff (Section 3.2 and 3.4), characterization and prediction of snow-water resources from climate models (Section 3.3). The method was also used in the development of a prototype real-time estimation method (Section 3.5).

**Figure 11: Seasonal and Interannual Variability in Rangewide Snow-Water Equivalent**



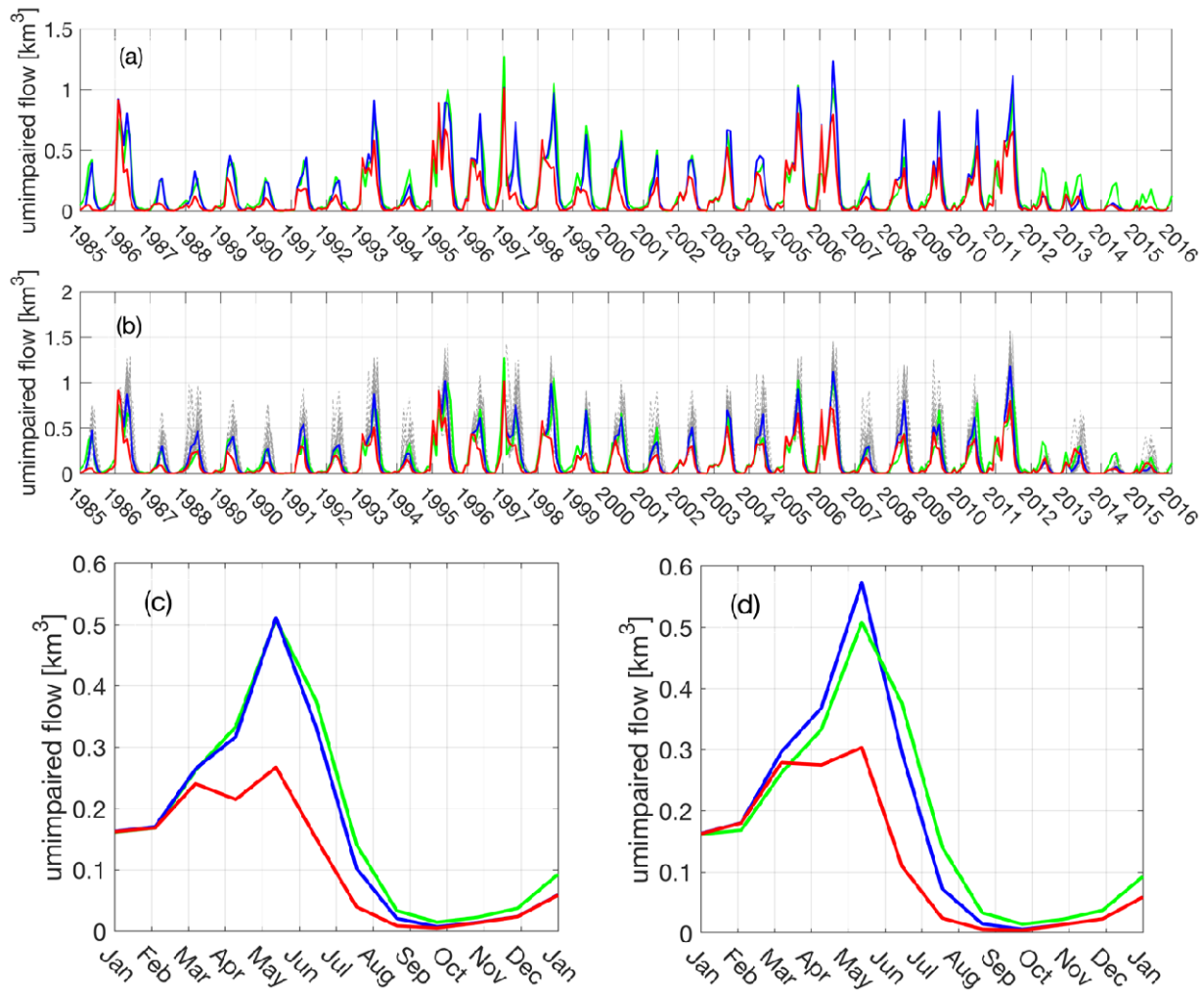
Daily time series of range-wide SWE (in km<sup>3</sup>) for each year of the SNSR record. The 'x' symbols mark the timing of the peak range-wide SWE for each year and the corresponding text indicates the value of peak SWE. Above- and below-average values are shown in white and black text respectively. The red line corresponds to April 1.

Source: University of California, Los Angeles

### 3.2 Testing the Effect of Improved Snow Estimates on Runoff Forecasts

To assess the potential for improving streamflow forecasts (and thereby hydropower forecasts) via SWE re-initialization, a hindcasting approach was used for the watersheds that are forecast by the California Department of Water Resources (DWR), as shown in Figure 4. Three cases were compared: 1) a baseline modeling case with default snow estimates, 2) a “perfect” forecast where SWE was re-initialized using the SNSR estimates at the time of peak SWE and forced with known deterministic meteorological forcing inputs, and 3) an ensemble streamflow prediction (ESP) case re-initialized using the SNSR estimates, but forced with unknown probabilistic meteorological forcing inputs. The three cases were examined for all watersheds with sample results for the Merced River watershed shown in Figure 12.

**Figure 12: Streamflow Forecast Comparison for Merced River**

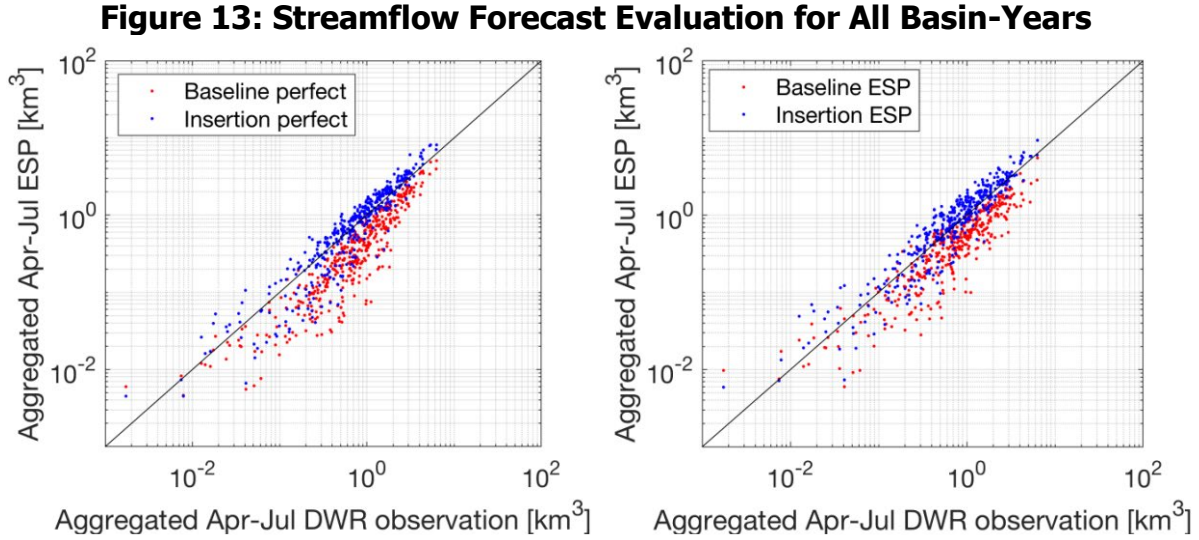


Comparison of the monthly streamflow from the SNSR insertion experiment (blue) and the baseline experiment (red) with the DWR streamflow observations (green) using the Merced River basin experiment results. (a) shows the comparison of the time-series streamflow from the perfect forecast experiment, (b) shows the comparison of the time-series streamflow from ESP, (c) and (d) show the average monthly streamflow over the study period from the perfect forecasting and ESP, respectively, relative to the baseline case and observations.

Source: University of California, Los Angeles

The results show a clear improvement in streamflow over the baseline case for both the perfect forecast and ESP cases relative to the observed (naturalized) streamflow.

Figure 13 shows the results for the baseline versus perfect and ESP forecasts relative to observed streamflow for all basin-years over the study period. There is generally significant improvement over the baseline when the more accurate SNSR SWE is used for re-initialization. The SWE insertion forecast was also compared to the DWR forecast system.



**Comparison of aggregated April–July streamflow from insertion experiment and baseline experiment for the (left) perfect forecast and (right) ESP forecast. Each dot in scatterplots represents aggregated streamflow for a single year at one gage; all dots represent the data from all 13 basins over all 31 years.**

Source: University of California, Los Angeles

Figure 14 shows a comparison of both forecasts to the observed streamflow.

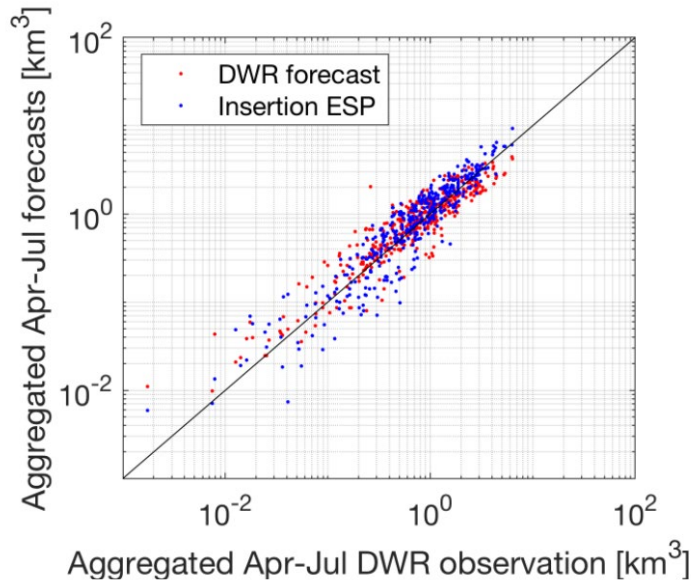
To quantify the improvement of the SNSR SWE insertion over a reference streamflow forecast, two metrics are defined:

$$NIC_{RMSE} = \frac{RMSE_R - RMSE_I}{RMSE_R} \quad (3.1)$$

$$NIC_{NSE} = \frac{NSE_I - NSE_R}{1 - NSE_R} \quad (3.2)$$

where  $RMSE_R$  and  $RMSE_I$  are the RMSE of the streamflow forecast from the reference experiment and the insertion experiment, respectively, and  $NSE_B$  and  $NSE_I$  are the Nash Sutcliffe Efficiency (NSE) of the streamflow forecast from the reference experiment and the insertion experiment, respectively. In both cases the normalized information content (NIC) essentially measures the relative RMSE and NSE difference between the reference forecast and the insertion forecast. Based on its definition, NIC values range from negative infinity to 1; positive NIC indicates the insertion improves the accuracy over the reference forecast, while negative NIC indicates the insertion results degrade with respect to the reference. The closer the NIC is to 1, the larger improvement the insertion forecast introduces.

**Figure 14: Streamflow Forecast Comparison for All Basin-Years Compared to Operational Forecasts**

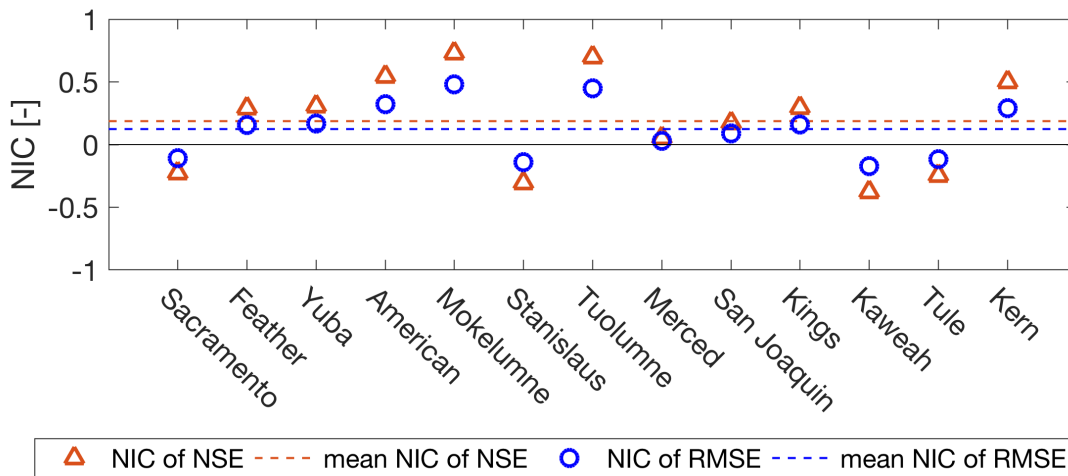


Comparison of seasonal streamflow forecast from peak-annual SWE insertion experiment with that from the DWR forecast issued at the peak-SWE month. Each dot represents the aggregated April–July streamflow for one gage for a single year.

Source: University of California, Los Angeles

The bulk improvement metrics are shown in Figure 15. In eight of the 13 basins, the SWE re-initialization shows an improved forecast over the reference DWR forecast system. Finally, the forecast systems were compared in dry years, when streamflow forecasts are most important. For the years in the driest 20 percent over the record examined, forecasts for all 13 basins were better for the SWE reinitialization over the standard DWR forecast (Figure 16), with a mean forecast improvement of 23 percent.

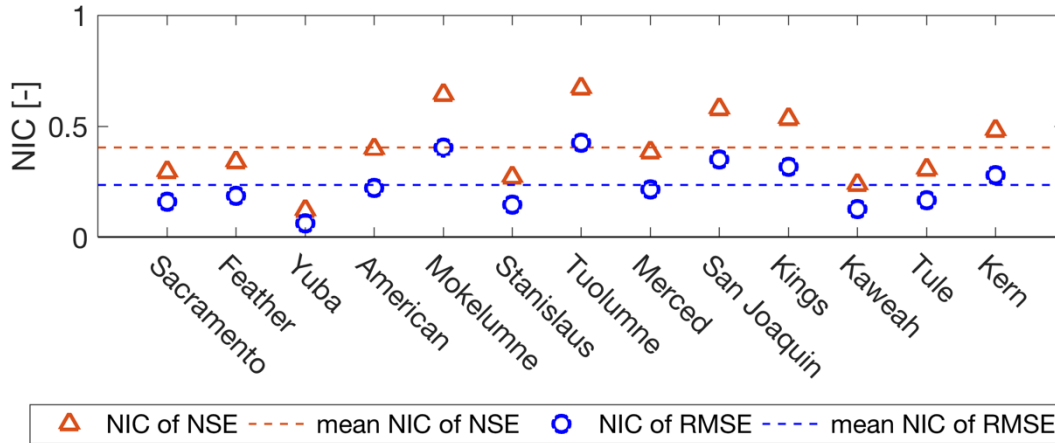
**Figure 15: Forecast Improvement Relative to Operational Forecasts**



The normalized information content (NIC) of RMSE (blue circle) and NIC of NSE (orange triangle) of the insertion ESP forecast made on DWR forecasting dates relative to the DWR forecasts on corresponding dates. Basins are ordered from north (left) to south (right).

Source: University of California, Los Angeles

**Figure 16: Forecast Improvement Relative to Operational Forecasts in Dry Years**



The NIC of RMSE (blue circle) and NIC of NSE (orange triangle) of the insertion ESP forecast made on DWR forecasting dates relative to the DWR forecasts on corresponding dates for the driest 20 percent of the years in the study period. Taken over all forecast points, the SWE insertion increases the accuracy of the April – July streamflow forecast by 23 percent.

Source: University of California, Los Angeles

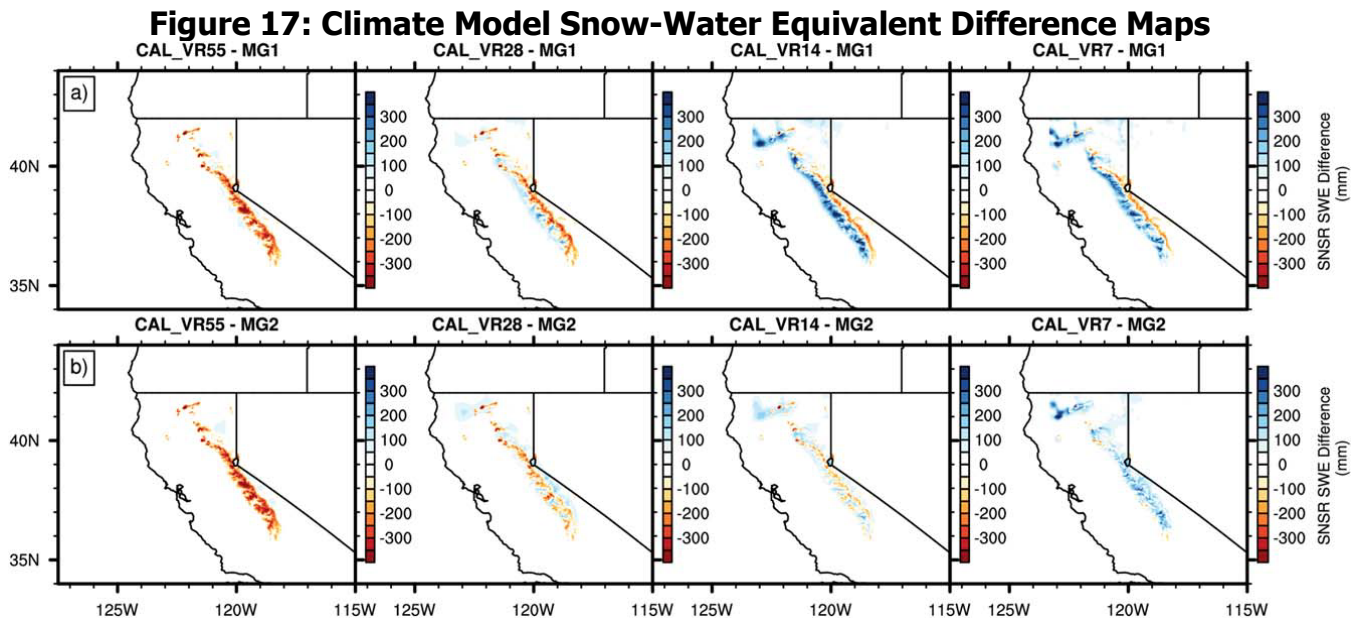
The results of this study (more details of which can be found in Li et al., 2019a) demonstrate that a SWE dataset that has sufficient accuracy in the magnitude and spatial distribution of basin-scale SWE has significant potential for improving streamflow forecasts. Accurate snow information itself (that is, initial conditions near peak SWE) was shown to be enough to allow physically based forecasts to have similar accuracy with a widely used statistical forecasting approach. These results also support the long-term efforts of the hydrologic community to continue to work toward developing near-real-time estimates of SWE (at high spatial and temporal resolution), through a combination remote sensing, reanalysis, machine learning, and other methods under consideration, in support of the larger goal of improved streamflow forecasts in snow dominated areas.

### 3.3 Evaluation of Climate Models in Representing Sierra Nevada and Western United States Snowpack Estimates

#### 3.3.1 Variable-Resolution Community Earth System Model

To assess the ability for simulating SWE in the Sierra Nevada, the SNSR was used for verifying the VR-CESM model as described in Section 2.3.1. The distribution of precipitation and partitioning of rain/snow on the windward and leeward side of the Sierra Nevada is critical when climate data are used for the assessment of watershed scale basins, particularly for ecosystem maintenance and reservoir operations. To assess the efficacy of variable resolution (VR) simulations over California (CAL\_VRXX where “XX” corresponds to the model resolution) in their representation of mountain snowpack (that is, rain and snow partitioning), Figure 17 highlights the December, January, February (DJF) climate average differences in SWE against SNSR. The CAL\_VR55 MG1 and MG2 simulations underestimate DJF climate SWE by 54.4 to 265.4 mm in the California mountain region as precipitation failed to transition from liquid to ice due to unrealistic topography and a smaller orographic uplift. For the CAL\_VR\_28 simulations, it is clear that the windward/leeward precipitation bias in MG1 shaped the windward/leeward snow bias (Figure 17). The DJF climate average SWE was 227.4 to 24.2

mm in the CAL\_VR MG1 simulations and 222.0 to 26.1 mm in the CAL\_VR MG2 simulations. The average absolute difference for SWE was 26.0 mm for CAL\_VR MG1 at horizontal grid-refinement of 28 km and improved to 17.2 mm for CAL\_VR MG2 at horizontal grid-spacings of 28 km, although benefits were most seen at 14 km (Figure 17). In terms of the DJF seasonal Pearson pattern correlation coefficients for SWE, the CAL\_VR MG1 simulations ranged between 0.28 and 0.68 when compared with SNSR. The CAL\_VR MG2 simulations generally improved upon the CAL\_VR MG1 simulations' DJF seasonal spatial correlations for SWE by 10.17 to 10.18 with values as high as 0.87, which were for CAL\_VR7 MG2. The windward/leeward ratios of CAL\_VR MG1 simulations highlight the poor distribution of SWE in the California mountain region with average windward/leeward ratios 4.6 times higher than SNSR. In contrast, the CAL\_VR MG2 simulations generally matched the mountain windward/leeward ratios of SNSR SWE (2.22) with ratios ranging between 0.92 and 1.12 for snow cover and between 1.27 and 1.96 for SWE.



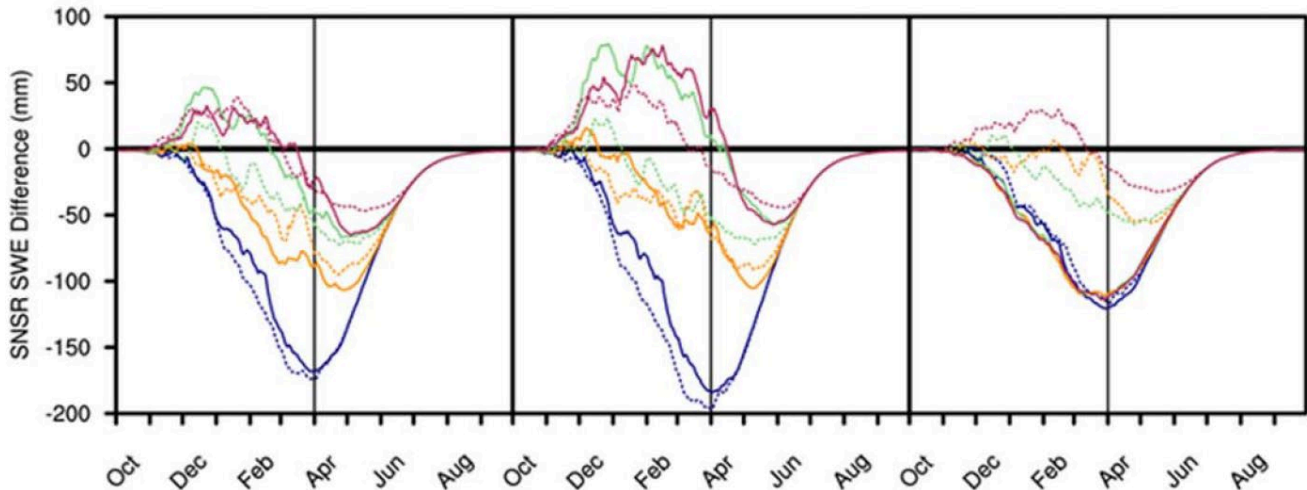
**Difference in modeled SWE against SNSR SWE. Results are shown for the eight CAL\_VR simulations at various refined horizontal grid-resolutions (55 7 km) using (a) MG1 versus (b) MG2 microphysics.**

Source: University of California, Los Angeles

Model efficacy in SWE over an average water year is depicted in Figure 18. Each of the plotted lines represents a given CAL\_VR simulation day averaged across the 16 simulated years and differenced from that of the reference data set for model evaluation in SWE. Results indicated that too much of the precipitation fell as rain versus snow. This results in the highest daily climate difference in average (range) simulated SWE accumulation for the windward, 261.5 to 269.1 mm (183–196 mm), and leeward, 237.0 to 239.9 mm (118–120 mm), side of the Sierra Nevada when compared with SNSR. At 28 km a clear SWE improvement is apparent with the average improved by 4.2 times in MG1 and 3.7 times in MG2 along the windward side of the Sierra Nevada. Further improvement arises in MG2 simulations on the leeward side of the Sierra Nevada by 3.5 times. Regardless of the resolution improvement beyond 28 km, a clear bias is present in most of the MG1 simulations with too much (too little) SWE accumulating prior to 1 April on the windward (leeward) side of the Sierra Nevada. This results in an average difference in the CAL\_VR MG1 simulations (at 28 km) of 15.4 mm on the windward

side of the Sierra Nevada and 40.0 mm on the leeward side of the Sierra Nevada. The CAL\_VR MG2 simulations at 28 km show a steady improvement in SWE from 28 to 7 km with the closest match to SNSR from October–March in the windward side of the Sierra Nevada. However, factors that influence the spring melt season led to a large underestimation of SWE (Figure 18). Although biased throughout the water year, the CAL\_VR7 MG2 simulation represents the closest approximation to SNSR in both the windward (−0.55 mm) and leeward (−1.69 mm) side of the Sierra Nevada. Thus, increased grid-refinement coupled with prognostic treatment of precipitation in the microphysics scheme did create major benefits in the seasonal cycle of mountain SWE over a given simulated water year.

**Figure 18: Climate Model Seasonal Snow-Water Equivalent Differences**



Water year daily climate average differences between the CAL\_VR MG1 (solid line) and CAL\_VR MG2 (dotted line) simulations at a maximum VR grid-spacing of 55 km (blue), 28 km (orange), 14 km (green), and 7 km (maroon). Simulations were compared against SNSR SWE for (left column) the full California Mountain Region, (middle column) windward side of the Sierra Nevada, and (right column) leeward side of the Sierra Nevada. The vertical black line represents the date of 1 April, which traditionally delineates the snowpack accumulation period from the melt period.

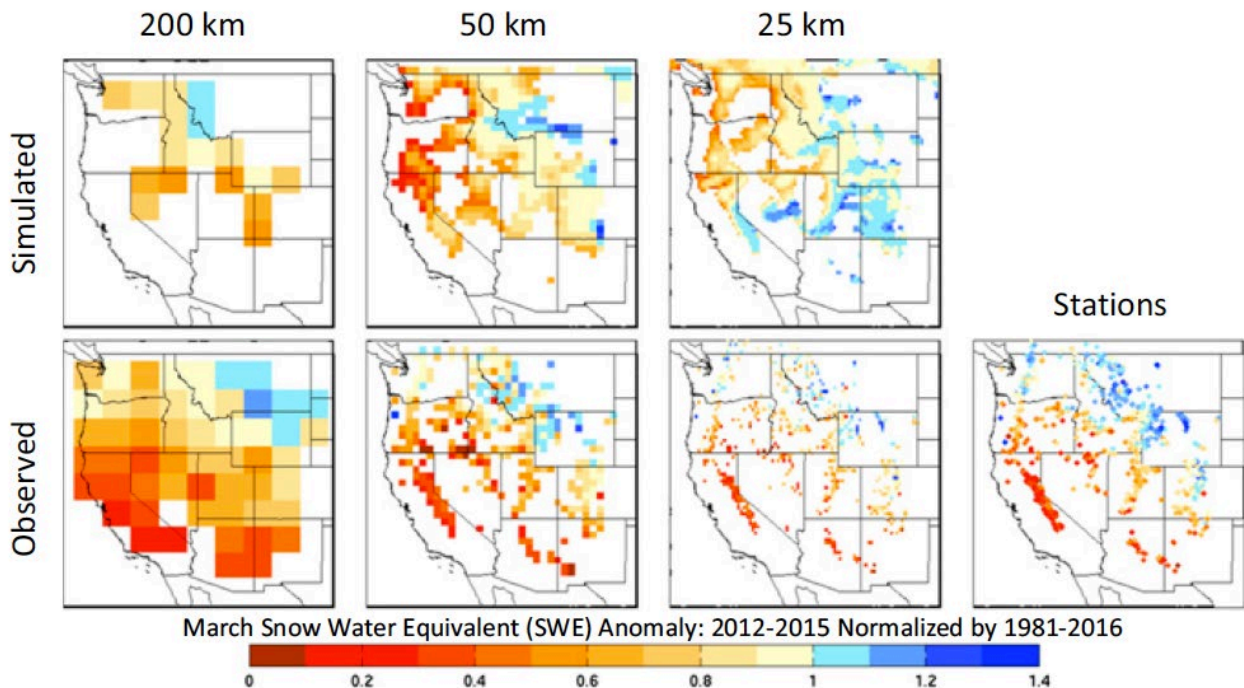
Source: University of California, Los Angeles

### 3.3.2 Geophysical Fluid Dynamics Laboratory Atmosphere-Ocean General Circulation Modeling Framework

Given the importance of snow-derived runoff, there is significant economic value in long-lead forecasts of SWE. In this study, the ability to predict SWE over the Western United States at long lead times (about eight months) was examined using the GFDL model applied at varying spatial resolutions (Section 2.3.2). The multiresolution modeling framework clearly illustrates the role of horizontal resolution for improving simulation of snowpack climatology (Figure 6 and Figure 19). At 200 km, mountains are smooth and low, resulting in minimal SWE confined to the interior Western United States. At 50 and 25 km, the models reproduce finer-scale maritime mountain features with SWE values approaching observations. Biases in the absolute value of snowpack are partially limited by resolution restricting topographic height and therefore snow accumulation. As a result, snowpack anomalies normalized by regional means were used to provide a relative comparison across resolutions. Figure 19 provides an example for the recent 2012–2015 multiyear southern Western United States snowpack drought. All of

the AOGCMs roughly reproduce the observed pattern of anomalously low snowpack in the southwest. The 50-km model appears to perform the best, while the 25-km model incorrectly predicts highs in the southern portion of the Western United States.

**Figure 19: Climate Model Snow-Water Equivalent Over Western United States (2012 - 2015)**



As in Figure 6, observed (bottom) and mean of annual ensemble mean simulated AOGCM March predictions from previous July (top) of snowpack anomalies in 2012-2015 relative to 1981-2016 mean. Note that for simulated plots, points have been masked for only those with climatological (1981-2016) simulated SWE greater than or equal to 1 cm.

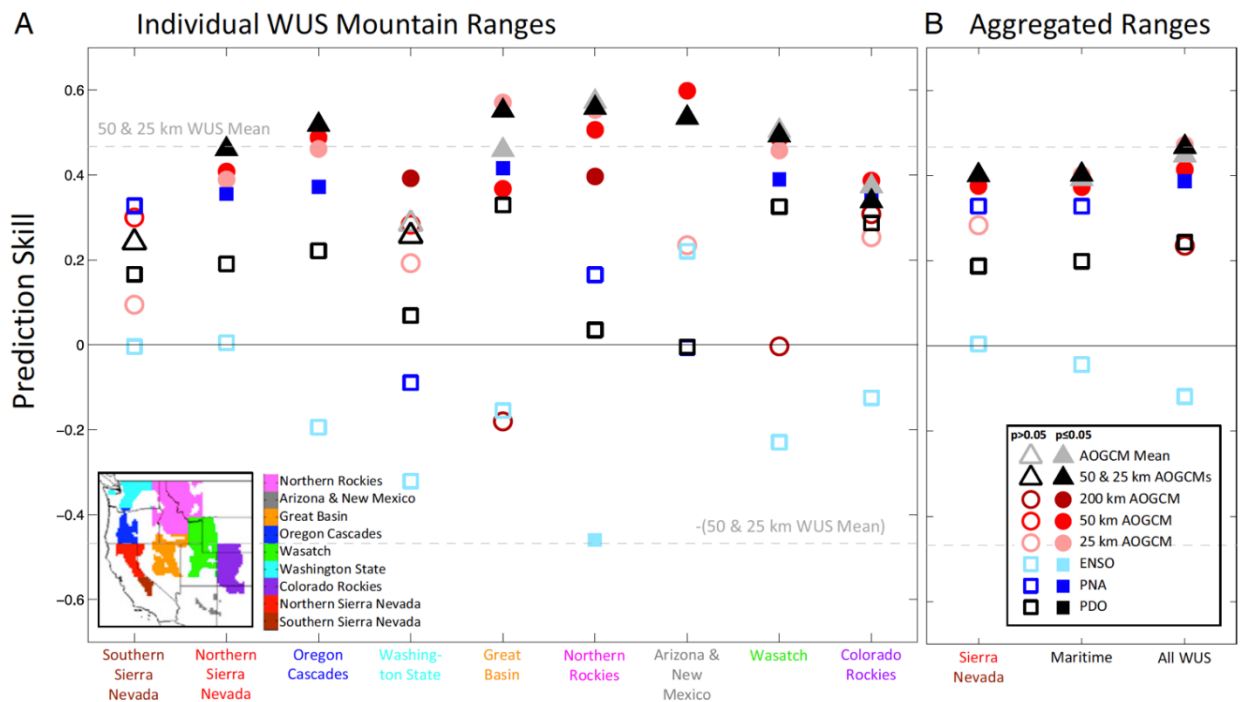
Source: University of California, Los Angeles

Figure 20 provides regional seasonal prediction metrics for AOGCM March snowpack based on previous July 1 initialization. The higher-resolution AOGCMs consistently produce positive statistically significant correlations across all regions except in the southern Sierra Nevada and in the State of Washington. The southern Sierra Nevada, being a narrow mountain range with the highest peak in the contiguous United States, Mt. Whitney, seems to require even higher resolutions than the GFDL system to achieve mountain heights for sufficient orographic precipitation and cold temperatures for snowpack dynamics. This region is characterized by narrow and infrequent storms—fewer than 10 per year, with some years receiving the majority of snowpack from a single storm (Huning and Margulis, 2017). The higher resolution models capture the spatial patterns of interannual variability, but with lower magnitudes than in the observations. This high natural variability and bias in the models may make it inherently more difficult to predict Sierra Nevada snowpack, particularly if the few storms that happen in a year are shifted outside the defined region.

To test larger-scale prediction skill and reduce errors caused by spatial differences in storms shifted across the region, aggregation to the Sierra Nevada, Maritime Mountains (Sierra Nevada, Oregon Cascades, Washington state), and the entire Western United States region

are shown in Figure 20. Aggregation leads to dynamical predictions outperforming statistical predictions everywhere. With aggregation, skill emerges across the combined Sierra Nevada and Maritime Mountains. However, the AOGCM snowpack predictions lose statistical significance over the Sierra Nevada when longer-term trends were removed from the model predictions, resulting in a loss of prediction skill in the aggregated Maritime Mountains despite skill in Oregon and Washington. Hence, the predictive skill shown in Figure 20 for the Sierra Nevada and Maritime Mountains came from the models' ability to reproduce the longer-term trend of Sierra Nevada snowpack loss. This suggests that the AOGCM system cannot capture the internally forced natural variability of Sierra Nevada snowpack. More work is needed with dynamical AOGCMs and observing systems customized for the Sierra Nevada and more broadly to California to: 1) enhance regional prediction skill or 2) elucidate if longer lead times are unattainable due to the nature of Sierra Nevada snowpack. More detail is provided in Kapnick et al. (2018).

**Figure 20: Statistical Performance of Climate Model Prediction Skill**



Mountain range snowpack prediction skill measured by correlations (Spearman) between observed March snowpack and predictors available 1 July from AOGCM models (triangles, circles) or climate indices (squares). Shown for (a) various mountain ranges and (b) ranges aggregated in increasing scale. Dashed line provided for the value of the higher resolution multimodel (50 km and 25 km) prediction (0.48) for snowpack over the entire mountainous Western United States. Inset provided for ranges in highest resolution model; the 200 km model has no ranges for: Northern and Southern Sierra Nevada, Oregon Cascades, or Arizona and New Mexico.

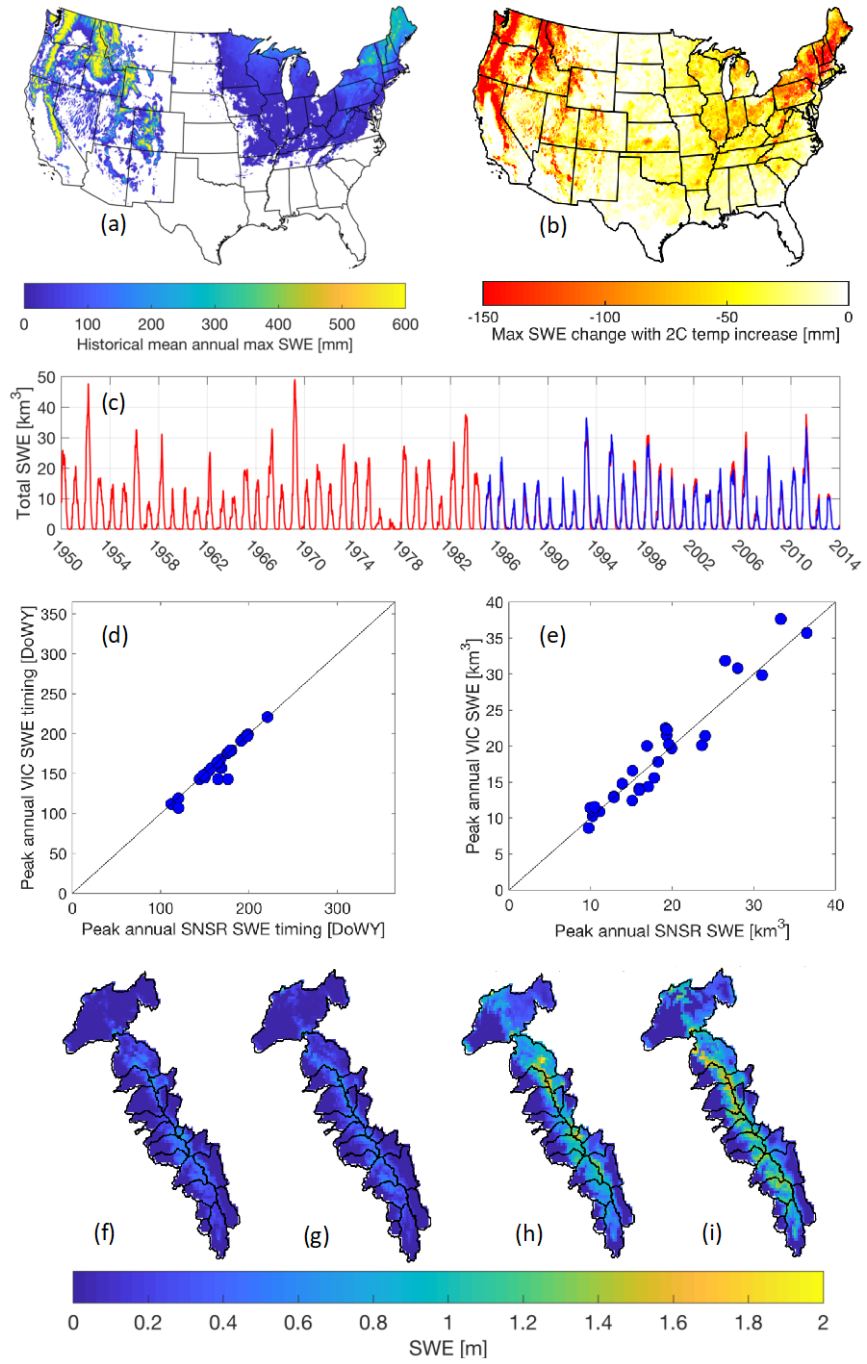
Source: University of California, Los Angeles

### 3.4 Role of Rain-on-Snow on Snowmelt-Driven Runoff in Current and Future Climates

As climate changes in snow-dominated areas, more precipitation events that might have previously fallen as snow will instead fall as rain. In this study, the project team used a

process-level characterization of historical and future ROS events, to quantify the source of runoff in large ROS events and the runoff contribution from ROS to extreme floods within the CONUS. Snow predictions from a hydrologic model were validated using the SNSR reanalysis (Figure 21).

**Figure 21: Verification of Snow-Water Equivalent in Rain-on-Snow Simulations**



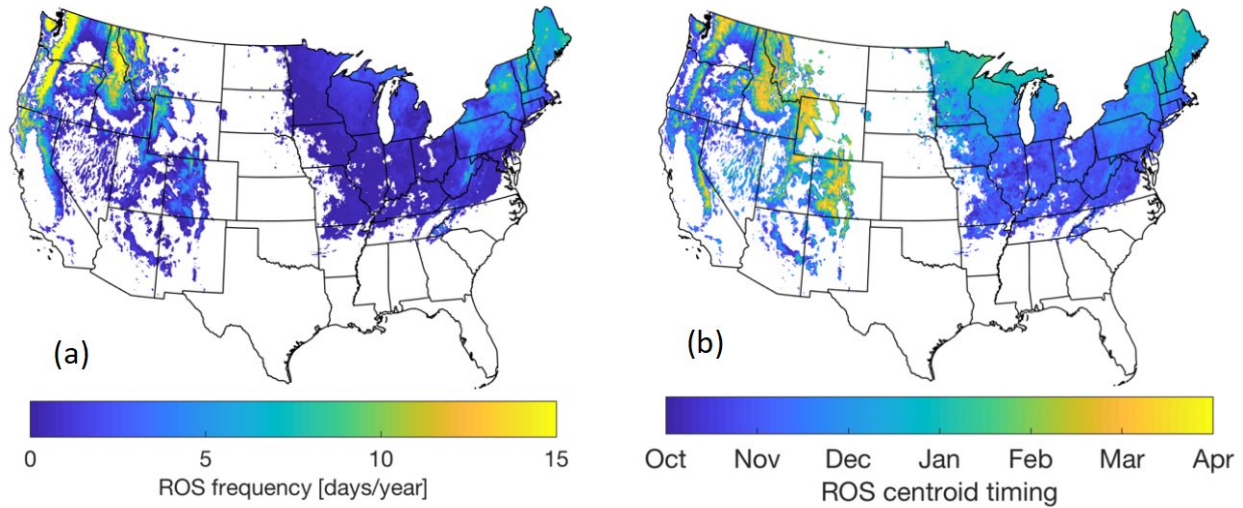
(a) Historical (1950–2013) simulated mean annual maximum SWE. (b) The change in the maximum SWE that would occur if the air temperature were uniformly increased over the 1950–2013 record by 2.0 degrees Celsius. (c) Comparison of the daily time series of total SWE (blue) in the Sierra Nevada from the SNSR dataset (Margulis et al., 2016) and from the VIC model (red). (d) Comparison of the timing and (e) the total volume of the annual peak SWE over the Sierra Nevada. (f) and (g) compare the spatial distribution of the peak SWE from the VIC model and from the SNSR (1990–lowest SWE WY). (h) and (i) are similar to (f) and (g), but for WY1993 (highest SWE WY).

Source: University of California, Los Angeles

The simulations indicate that the regions affected most heavily by ROS include the West Coast, the major mountain ranges of the western interior, the Upper Midwest, the Northeast, and the

lower Appalachians (Figure 22). While 70 percent of extreme runoff events in these regions is associated with ROS, the runoff generated during these ROS events accounts for less than 10 percent of the total extreme flood runoff; the much larger fraction of extreme runoff is derived either directly from intense rainfall or from clear-sky snowmelt. Rainfall is the dominant source of runoff in ROS events along the West Coast and over the west-facing slopes of the Cascades and Sierra Nevada, while snowmelt dominates the ROS runoff in the other regions in the CONUS.

**Figure 22: Historical Rain-on-Snow Event Characterization**

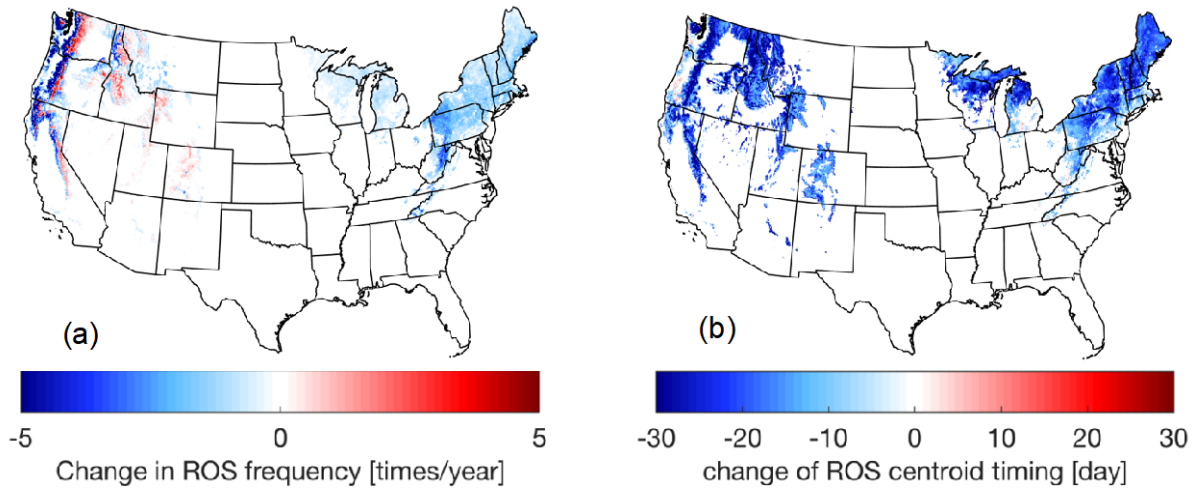


**(a) The frequency of historical ROS days. (b) The centroid of timing of all the historical ROS days. Results are shown only for grid cells with average maximum annual SWE greater than 20 mm.**

Source: University of California, Los Angeles

Historically, the role of ROS in streamflow extremes is most significant in mid-elevation areas, but based on the future climate simulations performed, this “significant influence zone” will shift to higher elevations in a warmer future. ROS will account for more of the extreme runoff in the high elevations of the mountainous West and the Upper Midwest, but less in areas with low and moderate elevations in the West and almost the entire East (Figure 23). The future ROS frequency changes exert a first order control on the future change of the runoff contribution from ROS to extreme floods. A more detailed presentation of the results is described in Li et al. (2019b).

**Figure 23: Future Changes in Rain-on-Snow Events**



a) Change in ROS frequency in the +2 degrees Celsius warmer scenario in comparison with the historical ROS frequency. (b) Change in the centroid of timing of ROS days in the +2 degrees Celsius warmer climate in comparison with the historical ROS timing. The white areas either have historical mean annual maximum SWE less than 20 mm or no identified ROS days in the warmer climate due to reduced SWE.

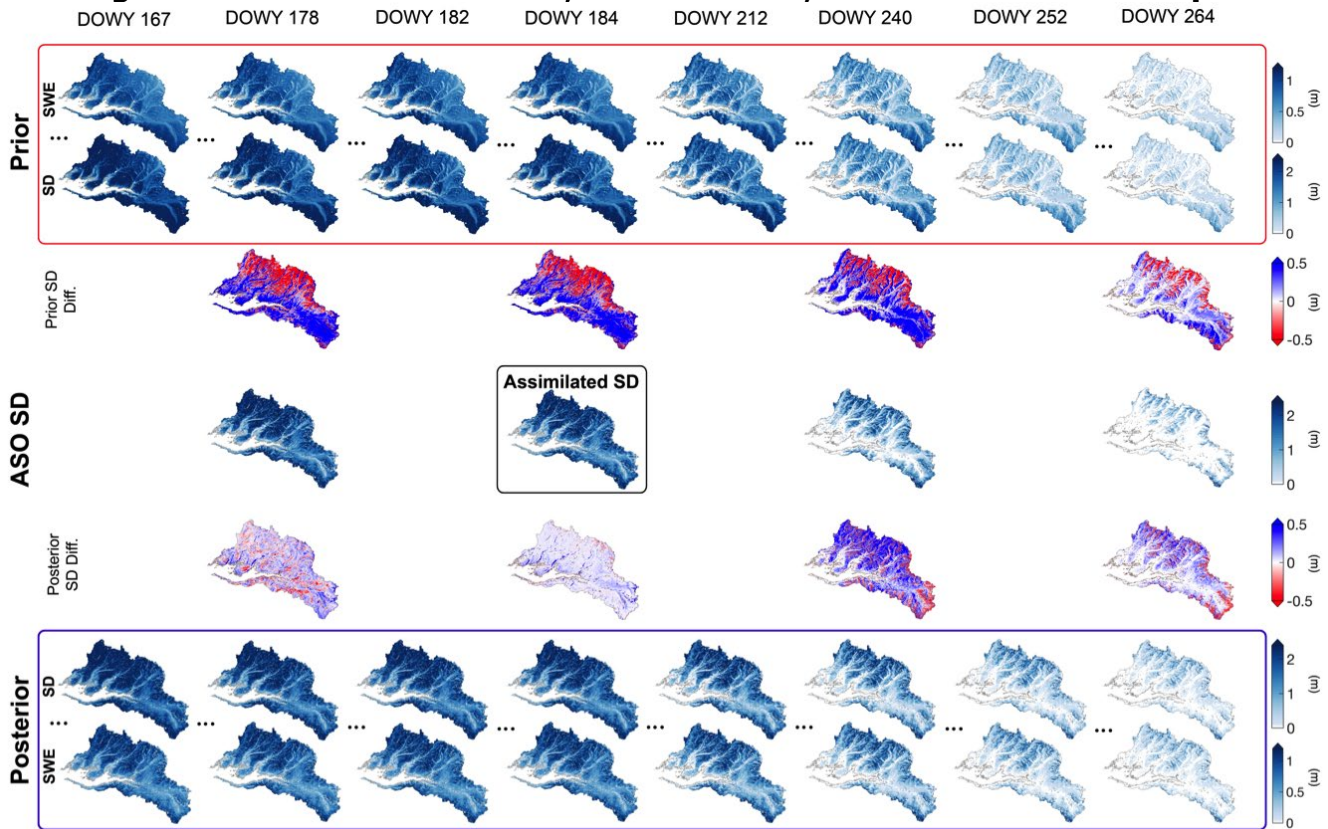
Source: University of California, Los Angeles

### 3.5 Examination of Real-Time Snow Estimation Method

In the final study of the project, the team examined the potential for real-time SWE and snowmelt estimation for driving streamflow in the context of assimilating the Airborne Snow Observatory (ASO) data into the reanalysis framework used to generate the SNSR. In particular, the goal of this work is to identify the potential for infrequent snow depth (SD) measurements to provide space-time continuous estimates of SWE.

Sample estimates from WY 2016 are presented in Figure 24 to qualitatively illustrate the results. The prior ensemble simulations provide daily SWE and SD estimates. The single assimilated ASO SD measurement is on DOWY 184, which is used to probabilistically condition the prior ensemble to generate the posterior estimate via the particle batch smoother update. The seasonal evolution of prior and posterior SD and SWE is shown, including on a subset of days with independent (that is, non-assimilated) ASO data (DOWY 178, 240, and 264). The posterior SD at the assimilation time (by construct) should closely match the measured SD field. This is clearly seen on DOWY 184, where the posterior SD and ASO SD fields are in good agreement, while different than the prior SD field. Importantly, the method essentially provides a retrieved (posterior) estimate of SWE via the relationship between modeled SWE and SD in the prior. The Bayesian smoother also implicitly uses SD information from the measurement time to generate the posterior estimates before and after the measurement day (that is, all daily estimates of SD and SWE are updated). As a result of the multitemporal ASO measurements, independent comparisons can be made between the posterior estimates and ASO data on days that were not used in the assimilation. It is evident that posterior SD fields on these days are also in better agreement with measurements than the prior (Figure 24).

**Figure 24: Illustration of Prior, Measurement, and Posterior Snow Depth**



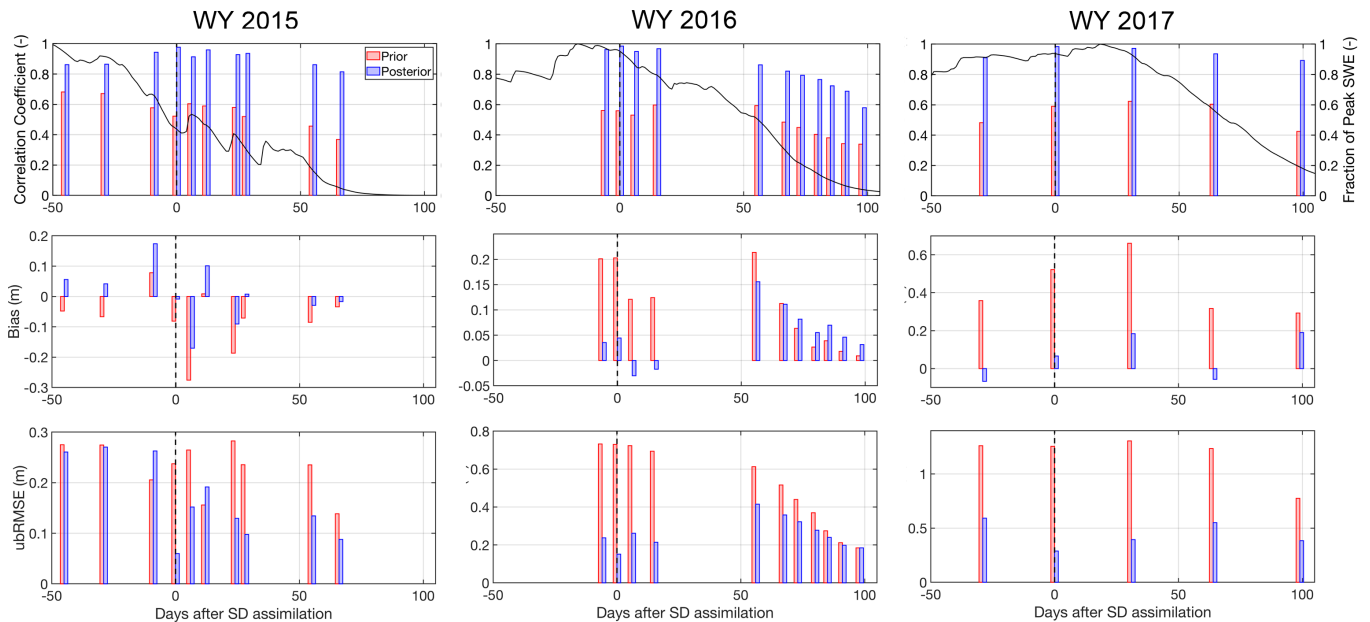
Sample estimation results from WY 2016, top two rows: prior (ensemble median) estimated SWE and snow depth (SD) fields on select days throughout the year; middle row: ASO measurements on four select days including the assimilation day (DOWY 184); bottom two rows: posterior (ensemble median) estimated SD and SWE fields resulting from the assimilation of the ASO measurement. Rows in between prior/posterior SD and ASO SD data show the respective SD difference fields on the day of assimilation (DOWY 184) and non-assimilation days (DOWYs 178, 240, 264).

Source: University of California, Los Angeles

Within a given WY, the posterior statistical metrics are expected to be optimal on the SD assimilation day. This is clearly seen in terms of the correlation, which is above 0.95 on the assimilation day for all three years tested (Figure 25, top row). The prior range (mean) of spatial correlation coefficients was: 0.37–0.60 (0.56), 0.34–0.60 (0.48), and 0.42–0.62 (0.54) in WYs 2015, 2016, and 2017, respectively. In comparison, the posterior range (mean) of spatial correlation coefficients was: 0.81–0.98 (0.91), 0.58–0.99 (0.83), and 0.89–0.98 (0.94). As expected, the correlation degrades away from the maximum values on the day of assimilation. For bias and unbiased RMSE, the optimal (lowest) values are also seen on the day of assimilation (Figure 25, middle/bottom rows) with intra-seasonal variability in their magnitudes due to: 1) the juxtaposition between the assimilated ASO measurement and the seasonal accumulation and ablation dynamics within each WY and 2) inter-annual variability due to the different snow accumulation amounts across WYs. The posterior bias and unbiased RMSE results mostly show sizeable improvements relative to the prior, with a few exceptions. The relative improvement is least in WY 2015 as a result of a few distinct factors: 1) less overall room for improvement due to the historically dry year, 2) the peak SWE occurring more than 50 days before the assimilated ASO measurement (compared to closer to peak SWE in WY 2016 and 2017), and 3) several relatively significant storms that occurred after the day of

ASO measurement assimilation (Figure 25, top left panel). Additionally, in WY 2016, while improvements are large near peak SWE, the prior and posterior SD bias and unbiased RMSE values are comparable to each other beyond about 75 days after the assimilated measurement.

**Figure 25: Estimation Errors in Snow Depth for All Measurement Times**



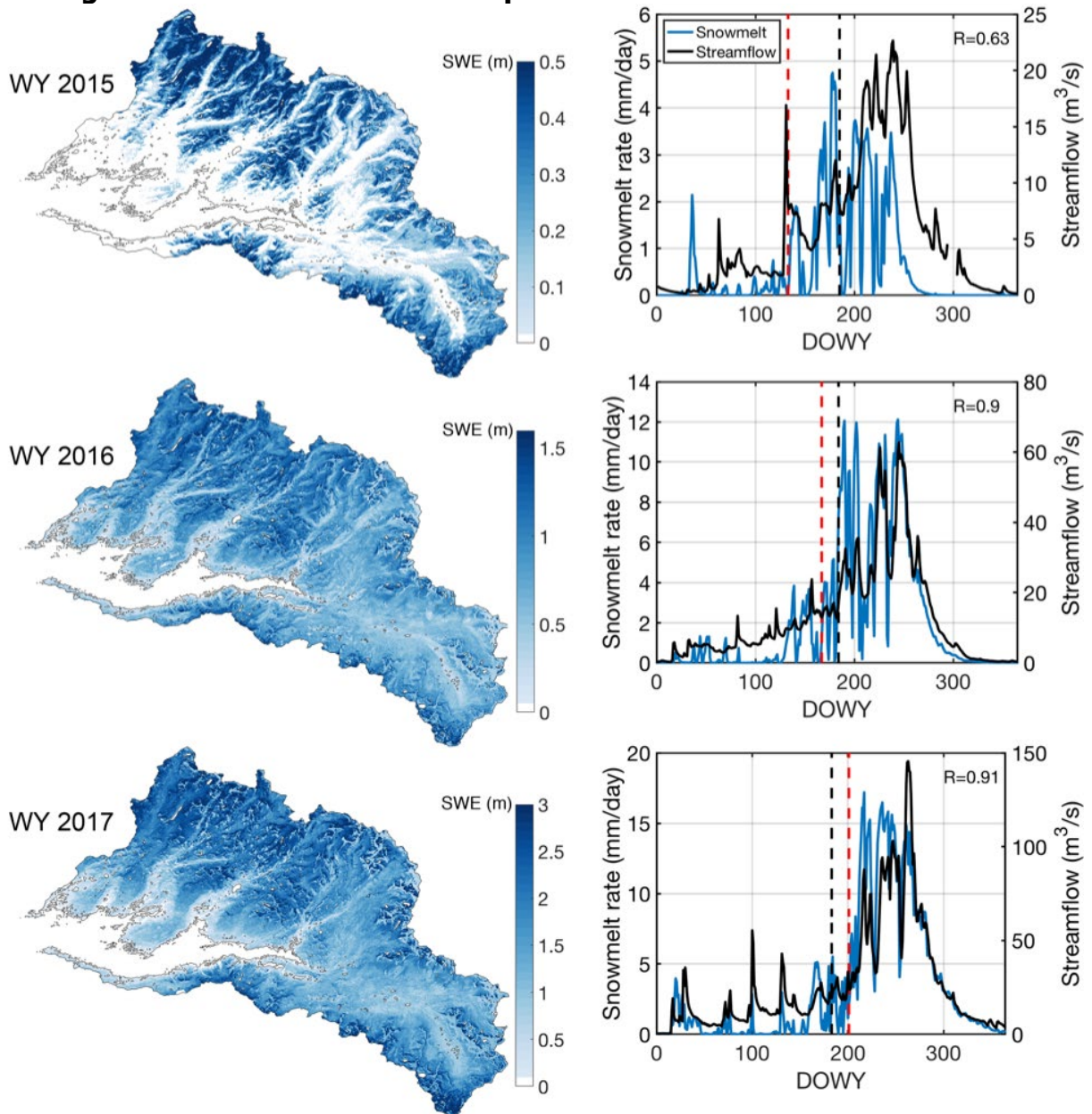
**Spatial statistics from the comparison of prior and posterior to ASO SD fields for the baseline case with assimilation of a single SD image, top row: correlation; middle row: bias; and bottom row: unbiased RMSE. In the top row, the fraction of (basin-average) peak SWE time series is shown for reference relative to ASO SD acquisition times. The vertical dashed line indicates the day of the assimilated SD measurement.**

Source: University of California, Los Angeles

A key benefit of the developed data assimilation framework is that non-observed posterior states and fluxes at non-observation times are provided. In fact, SD in and of itself is of less interest to hydrologists and water planners than other variables like peak accumulated SWE and snowmelt fluxes, which are more tightly linked to runoff and streamflow. This study provides a useful example whereby a variable that is more easily measured (SD) can be leveraged to generate other more useful state and flux estimates. To illustrate this, the posterior estimates of SWE fields at the time of peak basin-averaged SWE and the time series of snowmelt across the WY are shown in Figure 26. The peak SWE in WYs 2015 and 2016 occurs 52 and 17 days, respectively, before the day of SD assimilation, while in WY 2017 the peak SWE occurs 18 days after the day of assimilation. Based on this juxtaposition, the fraction of cumulative annual (posterior) snowmelt across each of the three WYs at the time of SD assimilation is 46 percent, 17 percent, and 11 percent respectively. The posterior estimates of snowmelt are also compared to the streamflow near the Tuolumne outlet (Figure 26, second column). The correlation coefficient between the daily basin-average snowmelt time series and the daily streamflow at the United States Geological Survey stream gage are respectively 0.63, 0.90, and 0.91 for WYs 2015, 2016, and 2017. The measured streamflow is the combined result of rainfall runoff, snowmelt-driven runoff, and baseflow and thus is not expected to be fully explained by the snowmelt time series alone, but the general agreement

provides additional, albeit indirect, verification of the posterior snow estimates. The fact that WY 2015 snowmelt is the least correlated with streamflow is not surprising due to the extremely early peak SWE relative to the day of SD assimilation and the fact that it was not only an extremely dry but also warm year (Margulis et al., 2016b), during which snow was stored only at much higher elevations relative to other years (Figure 26, left column), with a larger fraction of precipitation falling as rain and thus resulting in more rainfall-driven runoff. In the near-average year (2016) and wet year (2017), where snow is expected to dominate the runoff signal, there is a strong correlation between the posterior estimates and the measured streamflow.

**Figure 26: Peak Snow-Water Equivalent and Snowmelt Time Series**



(left column) Maps of estimated posterior SWE fields (in meters) for each WY on basin-averaged day-of-peak SWE. (right column) Posterior basin-average snowmelt time series compared to streamflow at watershed outlet (correlation between snowmelt and streamflow is shown in upper right corner of each panel). The SD data assimilation day and the day-of-peak SWE are shown with vertical dashed black and red lines respectively.

Source: University of California, Los Angeles

## **CHAPTER 4:**

# **Technology/Knowledge/Market Transfer Activities**

---

In this report, the research team developed a new snow-water equivalent dataset for analysis of snow-derived water resources over the Sierra Nevada in California. The new dataset was used in conjunction with modeling studies to characterize how snow-water equivalent, and therefore snow-derived runoff, can be improved. The dataset and model results are available to researchers and policy makers to provide better understanding historical and future availability of these resources. This project was part of a larger Department of Energy Clean Energy Research Center for Water-Energy Technologies project (<https://cerc-wet.berkeley.edu/>). As part of that larger effort the research team has participated in regular industry and stakeholder outreach efforts (<https://cerc-wet.berkeley.edu/events>) where results have been presented to a wide audience. The analysis is informative to policy makers and stakeholders for future climate adaptation plans on how these changes in snow-derived runoff will project to changes in hydropower production and how it can be optimally managed. The researchers will continue to work with the CEC and other stakeholders to inform them based on the analysis in this report.

# CHAPTER 5:

## Conclusions and Recommendations

---

In this report, the research team showed the potential for new methods for characterizing the Sierra Nevada snowpack and snow-derived runoff (both historically and in real-time) as well as how snow-derived runoff is likely to change in a warming climate. This was done through development of a new snow dataset that was used in conjunction with follow-on modeling and estimation studies targeting specific questions related to snow characterization and how it is changing.

The key conclusions and recommendations of the report include the following:

1. The newly developed state-of-the-art Sierra Nevada Snow Reanalysis (SNSR) dataset, which is based on the use of retrospective remotely sensed fractional snow-covered area data over the Landsat 5-8 record, and compares favorably to in-situ data from more than 9,000 station-years. The new dataset provides a unique capability for investigating snow processes at a space-time resolution, temporal extent, and accuracy not available from other existing datasets. Results provide an accounting of average annual snow-water equivalent and inter-annual variability over both the full Sierra Nevada and basins within it. One key implication of the SNSR dataset is its ability to validate other (that is, climate) models and initialize models to assess how improved snowpack states propagate to downstream estimates. The SNSR is currently available for public use, and the development of a Western United States-wide version of the reanalysis dataset is currently in progress.
2. To move toward better streamflow forecasting frameworks, a commonly applied model (VIC) was used but with re-initialized snow variables from the SNSR. When re-initialized with a realistic snow state (from the SNSR) near the time of peak snowpack water storage, significant improvements in streamflow forecasts were seen. Re-initialization of the annual peak snow-water equivalent increased the accuracy of the seasonal streamflow forecasts over operational statistical forecasts with an overall increase in accuracy of 13 percent. Seasonal streamflow forecast comparisons for earlier re-initialization for the driest years in the study period increase in early-season forecast accuracy across all basins with an overall increase of 23 percent. These improvements using historical data and a hindcasting approach imply that developing methods for real-time snow-water equivalent estimation would pay significant dividends on streamflow (and therefore) hydropower forecasts.
3. In two different climate modeling frameworks it was found that: 1) higher spatial resolution alone was insufficient to accurately predict snow distribution in space and time (compared to SNSR), but when combined with a prognostic cloud microphysics parameterization, significant improvements were seen; and 2) snowpack predictions with an eight-month lead time outperform statistical methods for the broader Western United States, but difficulties still exist at that time scale for the narrow Sierra Nevada. A key implication of this work is that climate models, when configured properly, have some skill in predicting Western United States snow distribution that could be exploited

for snow-water equivalent, runoff, and perhaps hydropower forecasts at short, medium, and even potentially long lead times, but that continued development of such models is needed in areas of complex terrain.

4. Simulations to characterize historical rain-on-snow over the conterminous United States showed that the sub-regions most affected by rain-on-snow are the major western mountain ranges (including the Cascades, the Sierra Nevada, and the Rockies) where extreme events are most likely in the spring. In a future (warmer climate) simulation, the role of rain-on-snow in local hydrologic extremes will increase in high-elevation mountains (greater than 2,000 meters), while decreasing at low and moderate elevation areas (less than 1,500 to 2,000 meters). Both results indicate the importance and potential amplification of extreme rain-on-snow events in the Sierra Nevada of California. Given this and the preceding results, using methods capable of characterizing events likely to generate rain-on-snow events (that is, atmospheric rivers) should be pursued for the purposes of predicting rain-on-snow events in the Sierra Nevada.
5. The same framework used in the development of the SNSR was used to assimilate lidar-derived snow depth measurements. Because snow depth has significant instantaneous correlation with snow-water equivalent, this method provided a mechanism for real-time characterization of snow-water equivalent and other non-observed variables (for example, snowmelt). In particular it can be concluded that even one measurement of snow depth around the time of peak snow-water equivalent (that is, typically about April 1) is capable of deriving useful estimates of snow-water equivalent and snowmelt as determined through comparison to independent observations. While the hydrologic and snow communities have been pursuing spatially distributed real-time estimates of snow-water equivalent for decades, this work provides an argument that using snow depth data (for example, from existing airborne or planned satellite platforms) combined with a data assimilation framework could make significant inroads toward the ultimate goal of a real-time snow-water equivalent estimation system. Other results from this project clearly show the benefits such a system would accrue.

## **CHAPTER 6:**

# **Benefits to Ratepayers**

---

Hydroelectric power generally depends on streamflow passing through run-of-river facilities or streamflow inputs to reservoirs behind dams that can be released to drive turbines. In either case, optimal management of these resources require optimal characterization and prediction of streamflow. In California, much of the hydroelectric power infrastructure exists in the Sierra Nevada where streamflow is driven by spring snowmelt. Because of the complex terrain in these environments, in-situ data is relatively sparsely distributed, yielding uncertainty in snow predictions where it is most needed. Moreover, previous models, which have been developed based on the in-situ data, are becoming less reliable as climate changes. Hence there is a need for better understanding of the Sierra Nevada snowpack and tools for real-time characterization and predictions at various forecast lead-times.

This project benefitted ratepayers by developing new datasets, analyses, and tools needed for improving forecasts of Sierra Nevada snowpack and the streamflow needed for hydropower at various lead times and how it is likely to change under long-term climate warming. Based on the conclusions and recommendations of this project, California is better equipped to optimize how snow-derived water and energy resources can be managed going forward. Developing and implementing such frameworks will have direct economic benefits by allowing for improvements in streamflow predictions and hydroelectric power forecasts and management.

## REFERENCES

- Bedsworth, Louise, Dan Cayan, Guido Franco, Leah Fisher, Sonya Ziaja. (California Governor's Office of Planning and Research, Scripps Institution of Oceanography, California Energy Commission, California Public Utilities Commission). 2018. Statewide Summary Report. California's Fourth Climate Change Assessment. Publication number: SUMCCCA4-2018-013.
- Cheng, L., A. AghaKouchak, E. Gilleland, and R.W. Katz. 2014. Non-stationary extreme value analysis in a changing climate. *Climatic Change*, 127(2), 353–369.  
<https://doi.org/10.1007/s10584-014-1254-5>
- Cortés, G., M. Girotto, S. Margulis. 2014. Analysis of minimum glacier and snow extent over the Andes using historical Landsat imagery, *Remote Sensing Environment*.  
<https://doi.org/10.1016/j.rse.2013.10.023>
- Delworth TL, et al. 2006. GFDL's CM2 global coupled climate models. Part I: Formulation and simulation characteristics. *Journal of Climate*, 19:643–674.  
<https://doi.org/10.1175/JCLI3629.1>
- Freudiger, D., I. Kohn, K. Stahl, and M. Weiler. 2014. Large-scale analysis of changing frequencies of rain-on-snow events with flood-generation potential. *Hydrology and Earth System Sciences*, 18(7), 2695–2709. <https://doi.org/10.5194/hess-18-2695-2014>
- Girotto, M., S.A. Margulis, and M. Durand. 2014a. Probabilistic SWE reanalysis as a generalization of deterministic SWE reconstruction techniques, *Hydrologic Processes*, 28, 3875–3895. <https://doi.org/10.1002/hyp.9887>
- Girotto, M., Cortés, G., Margulis, S. A., and M. Durand. 2014. Examining spatial and temporal variability in snow water equivalent using a 27-year reanalysis: Kern River watershed, Sierra Nevada. *Water Resources Research*, 50(8), 6713-6734.  
<https://doi:10.1002/2014WR015346>.
- Guan, B., N. Molotch, D. Waliser, S. Jepsen, T. Painter, and J. Dozier. 2013. Snow water equivalent in the Sierra Nevada: Blending snow sensor observations with snowmelt model simulations, *Water Resources Research*, 49, 5029–5046.  
<https://doi:10.1002/wrcr.20387>.
- Homer, C., J. Dewitz, J. Fry, M. Coan, N. Hossain, C. Larson, N. Herold, A. McKerrow, J.N. VanDriel, and J. Wickham. 2007. Completion of the 2001 national land cover database for the conterminous United States, *Photogrammetric Engineering and Remote Sensing*, 73(4), 337–341.
- Huning, L. S., and S.A. Margulis. 2017. Climatology of seasonal snowfall accumulation across the Sierra Nevada (USA): Accumulation rates, distributions, and variability, *Water Resources Research*, 53, 6033–6049, <https://doi.org/10.1002/2017WR020915>.

- Kapnick, S.B., X. Yang, G. Vecchi, T. Delworth, R. Gudgel, S. Malyshev, P.C.D. Milly, E. Shevliakova, S. Underwood, S. Margulis. 2018. Potential for Western United States Seasonal Snowpack Prediction, Proceedings of the National Academy of Sciences. <https://doi.org/10.1073/pnas.1716760115>
- Kumar, S. V., and Coauthors. 2014. Assimilation of remotely sensed soil moisture and snow depth retrievals for drought estimation. *Journal of Hydrometeorology*, 15, 2446–2469. <https://doi.org/10.1175/JHM-D-13-0132.1>
- Li, D., D.P. Lettenmaier, S.A. Margulis, K. Andreadis. 2019a. The value of accurate high-resolution and spatially continuous snow information to streamflow forecasts. *Journal of Hydrometeorology*. <https://doi.org/10.1175/JHM-D-18-0210.1>
- Li, D., D.P. Lettenmaier, S.A. Margulis, K.M. Andreadis. 2019b. The role of rain-on-snow events in the extreme floods over the conterminous United States, *Water Resources Research*. <https://doi.org/10.1029/2019WR024950>
- Liang, X., D.P. Lettenmaier, E.F. Wood, and S.J. Burges. 1994. A simple hydrologically based model of land surface water and energy fluxes for general circulation models. *Journal of Geophysical Research: Atmospheres*. 99(D7), 14415-14428. <https://doi.org/10.1029/94JD00483>
- Liston, G. E., 2004: Representing subgrid snow cover heterogeneities in regional and global models, *Journal of Climate*, 17(6), 1381–1397. [https://doi.org/10.1175/1520-0442\(2004\)017<1381:RSSCHI>2.0.CO;2](https://doi.org/10.1175/1520-0442(2004)017<1381:RSSCHI>2.0.CO;2)
- Liu, Y., C.D. Peters-Lidard, S.V. Kumar, K.R. Arsenault, and D.M. Mocko. 2015. Blending satellite-based snow depth products with in situ observations for streamflow predictions in the Upper Colorado River Basin. *Water Resources Research*, 51, 1182–1202, <https://doi.org/10.1002/2014WR016606>
- Livneh, B., E. A. Rosenberg, C. Lin, B. Nijssen, V. Mishra, K. M. Andreadis, E.P. Maurer, and D.P. Lettenmaier. 2013. Along-term hydrologically based dataset of land surface fluxes and states for the conterminous United States: Update and extensions. *Journal of Climate*, 26, 9384–9392, <https://doi.org/10.1175/JCLI-D-12-00508.1>
- Margulis, S., M. Giroto, G. Cortés, and M. Durand. 2015. A Particle Batch Smoother Approach to Snow Water Equivalent Estimation. *Journal of Hydrometeorology*, 16, 1752-1772, <https://doi.org/10.1175/JHM-D-14-0177.1>
- Margulis, S., G. Cortes, M. Giroto, and M. Durand. 2016a. A Landsat-era Sierra Nevada (USA) Snow Reanalysis (1985-2015). *Journal of Hydrometeorology*, <https://doi.org/10.1175/JHMD-15-0177.1>
- Margulis, S., G. Cortés, M. Giroto, L. Huning, D. Li, and M. Durand. 2016b. Characterizing the Extreme 2015 Snowpack Deficit in the Sierra Nevada (USA) and Implications for Recovery, *Geophysical Research Letters*, 43. <https://doi.org/10.1002/2016GL068520>

- Margulis, S.A., Y. Liu, E. Baldo, 2019a: A joint Landsat- and MODIS-based reanalysis approach for midlatitude montane seasonal snow characterization, *Frontiers in Earth Science* 7:272. <https://doi.org/10.3389/feart.2019.00272>
- Margulis, S.A., Y. Fang, D. Li, D.P. Lettenmaier, K. Andreadis. 2019b. The utility of infrequent snow depth images for deriving continuous space-time estimates of seasonal snow water equivalent. *Geophysical Research Letters*, <https://doi.org/10.1029/2019GL082507>
- Maurer, E. P., A. W. Wood, J. C. Adam, D. P. Lettenmaier, and B. Nijssen, 2002: Along-term hydrologically based dataset of land surface fluxes and states for the conterminous United States. *J. Climate*, 15, 3237–3251. [https://doi.org/10.1175/1520-0442\(2002\)015,3237:ALTHBD.2.0.CO;2](https://doi.org/10.1175/1520-0442(2002)015,3237:ALTHBD.2.0.CO;2)
- Melillo, Jerry M., Terese Richmond, and Gary W. Yohe, Eds. 2014. Highlights of climate change impacts in the United States: The Third National Climate Assessment. U.S. Global Change Research Program. 148 pp.
- Milly, P. C. D. and Betancourt, Julio and Falkenmark, Malin and Hirsch, Robert M. and Kundzewicz, Zbigniew W. and Lettenmaier, Dennis P. and Stouffer, Ronald J. Stationarity Is Dead: Whither Water Management? (2008). 5863, 573–574. <https://doi.org/10.1126/science.1151915>
- Painter, T. H., J. Dozier, D.A. Roberts, R.E. Davis, and R.O. Green. 2003. Retrieval of subpixel snow-covered area and grain size from imaging spectrometer data. *Remote Sensing of Environment*, 85(1), 64-77. [https://doi.org/10.1016/S0034-4257\(02\)00187-6](https://doi.org/10.1016/S0034-4257(02)00187-6)
- Rhoades, A. M., X. Huang, P.A. Ullrich, and C.M. Zarzycki. .2016. Characterizing Sierra Nevada snowpack using variable-resolution CESM. *Journal of Applied Meteorology and Climatology*, 55(1), 173–196. <https://doi.org/10.1175/JAMC-D-15-0156.1>
- Rhoades, A. M., P.A. Ullrich, and C.M. Zarzycki. 2017. Projecting 21st century snowpack trends in Western USA mountains using variable resolution CESM. *Climate Dynamics*, 50, 261–288. <https://doi.org/10.1007/s00382-017-3606-0>
- Rhoades, A. M., P.A. Ullrich, C.M. Zarzycki, H. Johansen, S.A. Margulis, H. Morrison, Z. Xu, and W. Collins. 2018. Sensitivity of mountain hydroclimate simulations in variable-resolution CESM to microphysics and horizontal resolution. *Journal of Advances in Modeling Earth Systems*, 10. <https://doi.org/10.1029/2018MS001326>
- Wood, A., T. Hopson, A. Newman, L. Brekke, J. Arnold, and M. Clark. 2016. Quantifying streamflow forecast skill elasticity to initial condition and climate prediction skill. *Journal of Hydrometeorology*, 17, 651–668. <https://doi.org/10.1175/JHM-D-14-0213.1>
- Xia, Y., et al. 2012. Continental-scale water and energy flux analysis and validation for the North American land data assimilation system project phase 2 (Nldas-2): 1. Intercomparison and application of model products, *Journal of Geophysical Research*, 117, D03109, <https://doi.org/10.1029/2011JD016048>

- Xue, Y., S. Sun, D. S. Kahan, and Y. Jiao. 2003. Impact of parameterizations in snow physics and interface processes on the simulation of snow cover and runoff at several cold region sites, *Journal of Geophysical Research*, 108(D22), 8859. <https://doi.org/10.1029/2002JD003174>
- Zarzycki, C. M., C. Jablonowski, D.R. Thatcher, and M.A. Taylor. 2015. Effects of localized grid refinement on the general circulation and climatology in the community atmosphere model. *Journal of Climate*, 28(7), 2777–2803. <https://doi.org/10.1175/JCLI-D-14-00599.1>